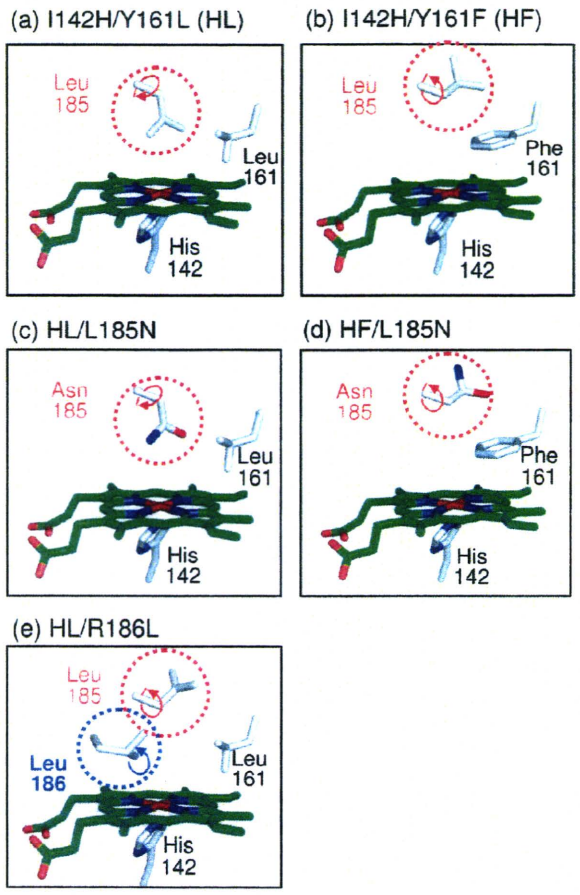

Figure 19. The proposed configuration of Leu-185 in (a) rHSA(HL)−heme and (b) rHSA(HF)−heme, Asn-185 in (c) rHSA(HL/L185N)−heme and (d) rHSA(HF/L185N)−heme, and Leu-186 in (e) rHSA(HL/R186L)–heme.

values were 1/6−1/11 of their former values. This corresponds to a free energy difference of −1.8 kcal mol^{-1} at 22 °C. The magnitude of the effect seems to be reasonable considering that, in HbO_2 and MbO_2, the distal His-64 stabilizes the coordinated O_2 by −0.6 to −1.4 kcal mol^{-1} because of the hydrogen bond (*187*). In contrast, The O_2 and CO binding parameters for rHSA(HF)−heme and rHSA(HF/L185N)−heme showed no significant differences. The bulky benzyl side chain of Phe-161 can prevent rotation of the polar amide group of Asn-185 and thereby decrease the effect of polarity and size on O_2 and CO binding parameters (Figure 19c,d) (*188*).

C. Substitution of Arg-186 with Leu or Phe. For administration into the human circulatory system, it would be better if the affinity were similar to the human RBC [$P_{50}(O_2)$: 8 Torr, 25 °C]. It is expected that providing a certain degree of hydrophobicity into the distal side of the heme by insertion of a nonpolar residue would reduce the O_2 binding affinity of the rHSA−heme complex. The most suitable position for that introduction might be at Arg-186, which is the entrance of the heme pocket and which is rather close to the central Fe(II) ion. Therefore, rHSA(HL/R186L)−hemin and rHSA(HL/R186F)−hemin were prepared. The O_2 dissociation rate constants of rHSA(HL/R186L)−heme and rHSA(HL/R186F)−heme were 3−4-fold higher than that of rHSA(HF)−heme, which reduced the O_2 binding affinities [larger $P_{50}(O_2)$]. This reduction might be attributable to the increased hydrophobicity in the distal pocket. The O_2 binding affinities of rHSA(HL/R186L)−heme [$P_{50}(O_2)$: 10 Torr] and rHSA(HL/R186F)−heme [$P_{50}(O_2)$: 9 Torr] have become equivalent to those of human RBC. The important structural factor in these mutants is Y161L, which enables the rotation of the isopropyl group of Leu-185 above the O_2 coordination site. Unexpectedly, the $k_{on}(O_2)$ and $k_{on}(CO)$ values of rHSA(HL/R186L)−heme and rHSA(HL/R186F)−heme were 3-fold and 3−4-fold higher than those of rHSA(HL)−heme and in the same range as that of rHSA(HF)−heme. In fact, Leu-161 is small, but the hydrophobic Leu-186 or Phe-186 might be integrated into the heme pocket from the entrance and might push up the neighboring Leu-185 residue (Figure 19e) (*188*).

We have engineered mutant rHSA−heme complexes that can bind O_2. Principal modifications to the heme pocket that are necessary to confer reversible O_2 binding are (i) replacement of Tyr-161 by hydrophobic amino acid (Leu or Phe), and (ii) introduction of His as a proximal base at position Ile-142. Furthermore, (iii) modification of the distal amino acid has a considerable effect on the modulation of O_2 and CO binding affinities.

4. CONCLUSIONS

The structures of our artificial O_2 carriers differ greatly from those of sophisticated RBCs. However, clear advantages of simplified artificial O_2 carriers are readily apparent: the absence of blood-type antigens and infectious viruses, stability for long-term storage at room temperature for any emergency, all of which overwhelm the functionality of RBCs. The shorter half-life of artificial O_2 carriers in the bloodstream (ca. 3 days) limits their use, but they are applicable as a transfusion alternative for shorter periods of use. Easy manipulation of physicochemical properties such as $P_{50}(O_2)$ and viscosity supports their possible development of tailor-made O_2 carriers to suit various clinical indications. The achievements of ongoing research described above give us confidence in advancing the further development with the expectation of its eventual realization.

ACKNOWLEDGMENT

The authors gratefully acknowledge Prof. H. Nishide, Prof. S. Takeoka (Waseda Univ.), Prof. R. Yozu, Prof. M. Suematsu, Dr. H. Horinouchi, Dr. M. Watanabe, Dr. E. Ikeda, Dr. Y. Izumi, Dr. M. Yamamoto, Dr. T. Ikeda (Keio Univ.), Dr. H. Ikeda, Dr. H. Azuma, Dr. M. Fujiwara, Dr. H. Abe (Hokkaido Red Cross Blood Center), Dr. M. Takaori (East Takarazuka Satoh Hospital), Prof. M. Otagiri (Kumamoto Univ.), Prof. M. Intaglietta (Univ. of California, San Diego), Prof. W. T. Phillips (Univ. of Texas, San Antonio), Prof. D. Erni (Inselspital Hospital, Univ. of Berne), Prof. M. Okamoto (Weill Med. College, Cornell Univ.), Prof. S. Curry (Imperial College London) and their active colleagues for meaningful discussions and contributions to this research. This work was partly supported by Health Sciences Research Grants (Research on Regulatory Science) from the Ministry of Health, Labour and Welfare, Japan, and Grant-in-Aid for Scientific Research from JSPS. The authors are the holders of patents related to the production and utilization of HbV and albumin−hemes.

LITERATURE CITED

(1) Perutz, M. F. (1970) Stereochemistry of cooperative effects in haemoglobin. *Nature 228*, 726–739.
(2) Jones, R. D., Summerville, A., and Basolo, F. (1979) Synthetic oxygen carriers related to biological systems. *Chem. Rev. 79*, 139–179.
(3) Collman, J. P. (1977) Synthetic model for the oxygen-binding hemoproteins. *Acc. Chem. Res. 10*, 265–272.
(4) Momenteau, M., and Reed, C. (1994) Synthetic heme dioxygen complexes. *Chem. Rev. 94*, 659–698.
(5) Collman, J. P., Gagne, R. R., Halbert, T. R., Marchon, J.-C., and Reed, C. A. (1973) Reversible oxygen adduct formation in ferrous complexes derived from "picket fence" porphyrins. A model for oxymyoglobin. *J. Am. Chem. Soc. 73*, 7868–7870.

(6) Collman, J. P., Gagne, R. R., Reed, C. A., Halbert, T. R., Lang, G., and Robinson, W. T. (1975) "Picket fence porphyrins." Synthetic models for oxygen binding hemoproteins. *J. Am. Chem. Soc. 97*, 1427–1439.

(7) Matsushita, Y., Hasegawa, E., Eshima, K., and Tsuchida, E. (1983) Synthesis of amphiphilic porphinatoiron complexes having phosphocholine groups. *Chem. Lett. 1983*, 1387–1389.

(8) Tsuchida, E. (1985) Liposome-embedded iron-porphyrins as an artificial oxygen carrier. *Ann. N.Y. Acad. Sci. 446*, 429–442.

(9) Tsuchida, E., and Nishide, H. (1986) Hemoglobin model - artificial oxygen carrier composed of porphinatoiron complexes. *Top. Curr. Chem. 1132*, 63–99.

(10) Komatsu, T., Moritake, M., Nakagawa, A., and Tsuchida, E. (2002) Self-organized lipid-porphyrin bilayer membranes in vesicular form: nanostructure, photophysical properties and dioxygen coordination. *Chem. Eur. J. 8*, 5469–5480.

(11) Komatsu, T., Ando, K., Kawai, N., Nishide, H., and Tsuchida, E. (1995) O_2-transport albumin - a new hybrid hemoprotein incorporating tetraphenylporphinatoiron(II). *Chem. Lett.* 813–814.

(12) Savitsky, J. P., Doczi, J., Black, J., and Arnold, J. D. (1978) A clinical safety trial of stroma-free hemoglobin. *Clin. Pharm. Ther. 23*, 73–80.

(13) Greenwald, R. B., Pendri, A., Martinez, A., Gilbert, C., and Bradley, P. (1996) PEG thiazolidine-2-thione, a novel reagent for facile protein modification: conjugation of bovine hemoglobin. *Bioconjugate Chem. 7*, 638–641.

(14) Kluger, R., and Li, X. (1997) Efficient chemical introduction of a disulfide cross-link and conjugation site into human hemoglobin at β-lysine-82 utilizing a bifunctional aminoacyl phosphate. *Bioconjugate Chem. 8*, 921–926.

(15) Sakai, H., Yuasa, M., Onuma, H., Takeoka, S., and Tsuchida, E. (2000) Synthesis and physicochemical characterization of a series of hemoglobin-based oxygen carriers: objective comparison between cellular and acellular types. *Bioconjugate Chem. 11*, 56–64.

(16) Hai, T. T., Pereira, D. E., Nelson, D. J., Catarello, J., and Srnak, A. (2000) Surface modification of diaspirin cross-linked hemoglobin (DCLHb) with chondroitin-4-sulfate derivatives. Part 1. *Bioconjugate Chem. 11*, 705–713.

(17) Manjula, B. N., Tsai, A., Upadhya, R., Perumalsamy, K., Smith, P. K., Malavalli, A., Vandegriff, K., Winslow, R. M., Intaglietta, M., Prabhakaran, M., Friedman, J. M., and Acharya, A. S. (2003) Site-specific PEGylation of hemoglobin at Cys-93(β): correlation between the colligative properties of the PEGylated protein and the length of the conjugated PEG chain. *Bioconjugate Chem. 14*, 464–472.

(18) Murray, J. A., Ledlow, A., Launspach, J., Evans, D., Loveday, M., and Conklin, J. L. (1995) The effects of recombinant human hemoglobin on esophageal motor function in humans. *Gastroenterology 109*1241–1248.

(19) Chatterjee, R., Welty, E. V., Walder, R. Y., Pruitt, S. L., Rogers, S. L., Arnone, A., and Walder, J. A. (1986) Isolation and characterization of a new hemoglobin derivative cross-linked between the a chains (lysine $99\alpha_1 \gg$ lysine $99\alpha_2$). *J. Biol. Chem. 261*, 9929–9937.

(20) Iwashita, Y. (1991) Pyridoxalated hemoglobin-polyoxyethylene conjugate (PHP) as an O_2 carrier. *Artif. Organs Today 1*, 89–114.

(21) Riess, J. G. (2001) Oxygen carriers ("blood substitutes") - raison d'etre, chemistry, and some physiology. *Chem. Rev. 101*, 2797–2920.

(22) de Figueiredo, L. F., Mathru, M., Solanki, D., Macdonald, V. W., Hess, J., and Kramer, G. C. (1997) Pulmonary hypertension and systemic vasoconstriction might offset the benefits of acellular hemoglobin blood substitutes. *J. Trauma 42*, 847–854.

(23) Tsai, A. G., Kerger, H., and Intaglietta, M. (1995) Microcirculatory consequences of blood substitution with $\alpha\alpha$-hemoglobin. In *Blood Substitutes: Physiological Basis of Efficacy* (Winslow, R. M., Vandegriff, K., Intaglietta, M., Eds.) pp155–174, Birkhauser, Boston.

(24) Goda, N., Suzuki, K., Naito, M., Takeoka, S., Tsuchida, E., Ishimura, Y., Tamatani, T., and Suematsu, M. (1998) Distribution of heme oxygenase isoforms in rat liver. Topographic basis for carbon monoxide-mediated microvascular relaxation. *J. Clin. Invest. 101*, 604–612.

(25) Sakai, H., Hara, H., Yuasa, M., Tsai, A. G., Takeoka, S., Tsuchida, E., and Intaglietta, M. (2000) Molecular dimensions of Hb-based O_2 carriers determine constriction of resistance arteries and hypertension. *Am. J. Physiol. Heart Circ. Physiol. 279*, H908–H915.

(26) Burhop, K., Gordon, D., and Estep, T. (2004) Review of hemoglobin-induced myocardial lesions. *Artif. Cells Blood Substit. Immobil. Biotechnol. 32*, 353–374.

(27) Neragi-Miandoab, S., and Vlahakes, G. J. (2006) Elevated troponin I level with hemoglobin based oxygen carrying solutions (HBOCs) as a priming solution despite improved left ventricular function. *Interact. Cardiovasc. Thorac. Surg. 5*, 135–138.

(28) Natanson, C., Kern, S. J., Lurie, P., Banks, S. M., and Wolfe, S. M. (2008) Cell-free hemoglobin-based blood substitutes and risk of myocardial infarction and death: a meta-analysis. *JAMA 299*, 2304–2312.

(29) Balla, J., Jacob, H. S., Balla, G., Nath, K., Eaton, J. W., and Vercellotti, G. M. (1993) Endothelial-cell heme uptake from heme proteins: induction of sensitization and desensitization to oxidant damage. *Proc. Natl. Acad. Sci. U.S.A. 90*, 9285–9289.

(30) Sakai, H., Sato, A., Masuda, K., Takeoka, S., and Tsuchida, E. (2008) Encapsulation of concentrated hemoglobin solution in phospholipid vesicles retards the reaction with NO, but not CO, by intracellular diffusion barrier. *J. Biol. Chem. 283*, 1508–1517.

(31) Sakai, H., Sato, A., Sobolewski, P., Takeoka, S., Frangos, J. A., Kobayashi, K., Intaglietta, M., and Tsuchida, E. (2008) NO and CO binding profiles of hemoglobin vesicles as artificial oxygen carriers. *Biochim. Biophys. Acta 1784*, 1441–1447.

(32) Martini, J., Cabrales, P., Tsai, A. G., and Intaglietta, M. (2006) Mechanotransduction and the homeostatic significance of maintaining blood viscosity in hypotension, hypertension and haemorrhage. *J. Intern. Med. 259*, 364–372.

(33) Sakai, H., Suzuki, Y., Kinoshita, M., Takeoka, S., Maeda, N., and Tsuchida, E. (2003) O_2 release from Hb vesicles evaluated using an artificial, narrow O_2-permeable tube: comparison with RBCs and acellular Hbs. *Am. J. Physiol. Heart Circ. Physiol. 285*, H2543–H2555.

(34) Vandegriff, K. D., and Olson, J. S. (1984) The kinetics of O_2 release by human red blood cells in the presence of external sodium dithionite. *J. Biol. Chem. 259*, 12609–12618.

(35) Chang, T. M. S. (2005) Therapeutic applications of polymeric artificial cells. *Nat. Rev. Drug Discov. 4*, 221–235.

(36) Toyoda, T. (1965) Artificial blood. *Kagaku 35*, 7–13 (in Japanese).

(37) Kimoto, S., Hori, M., Toyoda, T., and Sekiguchi, W. (1968) Artificial red cells. *Gekachiryou (Surgical Therapy) 19*, 324–332 (in Japanese).

(38) Bangham, A. D., and Horne, R. W. (1964) Negative staining of phospholipids and their structure modification by surface-active agents as observed in the electron microscope. *J. Mol. Biol. 8*, 660–668.

(39) Bangham, A. D., Standish, M. M., and Watkins, J. C. (1965) Diffusion of univalent ions across the lamellae of swollen phospholipids. *J. Mol. Biol. 13*, 238–252.

(40) Djordjevich, L., and Miller, I. F. (1977) Lipid encapsulated hemoglobin as a synthetic erythrocyte. *Fed. Proc. 36*, 567–571.

(41) Farmer, M. C., Rudolph, A. S., Vandegriff, K. D., Hayre, M. D., Bayne, S. A., and Johnson, S. A. (1988) Liposome-encapsulated hemoglobin: oxygen binding properties and respiratory function. *Biomater. Artif. Cells Artif. Organs 16*, 289–299.

(42) Rudolph, A. S., Klipper, R. W., Goins, B., and Phillips, W. T. (1991) In vivo biodistribution of a radiolabeled blood substitute: ^{99m}Tc-labeled liposome-encapsulated hemoglobin in an anesthetized rabbit. *Proc. Natl. Acad. Sci. U.S.A. 88*, 10976–10980.

(43) Phillips, W. T., Klipper, R. W., Awasthi, V. D., Rudolph, A. S., Cliff, R., Kwasiborski, V., and Goins, B. A. (1999) Polyethylene glycol-modified liposome-encapsulated hemoglobin: a long circulating red cell substitute. *J. Pharmacol. Exp. Ther. 288*, 665–670.

(44) Usuba, A., Osuka, F., Kimura, T., Sato, R., Ogata, Y., Gotoh, H., Kimura, T., and Fukui, H. (1998) Effect of liposome-encapsulated hemoglobin, neo red cells, on hemorrhagic shock. *Surg. Today 28*, 1027–1035.

(45) Yoshioka, H. (1991) Surface modification of haemoglobin-containing liposomes with polyethylene glycol prevents liposome aggregation in blood plasma. *Biomaterials 12*, 861–864.

(46) Sakai, H., Hamada, K., Takeoka, S., Nishide, H., and Tsuchida, E. (1996) Physical properties of hemoglobin vesicles as red cell substitutes. *Biotechnol. Prog. 12*, 119–125.

(47) Takeoka, S., Ohgushi, T., Terase, K., Ohmori, T., and Tsuchida, E. (1996) Layer-controlled hemoglobin vesicles by interaction of hemoglobin with a phospholipid assembly. *Langmuir 12*, 1755–1759.

(48) Sou, K., Naito, Y., Endo, T., Takeoka, S., and Tsuchida, E. (2003) Effective encapsulation of proteins into size-controlled phospholipid vesicles using freeze-thawing and extrusion. *Biotechnol. Prog. 19*, 1547–1552.

(49) Sakai, H., Takeoka, S., Yokohama, H., Seino, Y., Nishide, H., and Tsuchida, E. (1993) Purification of concentrated Hb using organic solvent and heat treatment. *Protein Expression Purif. 4*, 563–569.

(50) Abe, H., Ikebuchi, K., Hirayama, J., Fujihara, M., Takeoka, S., Sakai, H., Tsuchida, E., and Ikeda, H. (2001) Virus inactivation in hemoglobin solution by heat treatment. *Artif. Cells Blood Substit. Immobil. Biotechnol. 29*, 381–388.

(51) Chung, J., Hamada, K., Sakai, H., Takeoka, S., and Tsuchida, E. (1995) Ligand-exchange reaction of carbonylhemoglobin to oxyhemoglobin in a hemoglobin liquid membrane. *Nippon Kagaku Kaishi 2*, 123–127 (in Japanese).

(52) Takeoka, S., Sakai, H., Kose, T., Mano, Y., Seino, Y., Nishide, H., and Tsuchida, E. (1997) Methemoglobin formation in hemoglobin vesicles and reduction by encapsulated thiols. *Bioconjugate Chem. 8*, 539–544.

(53) Teramura, Y., Kanazawa, H., Sakai, H., Takeoka, S., and Tsuchida, E. (2003) Prolonged oxygen-carrying ability of hemoglobin vesicles by coencapsulation of catalase *in vivo*. *Bioconjugate Chem. 14*, 1171–1176.

(54) Sakai, H., Masada, Y., Onuma, H., Takeoka, S., and Tsuchida, E. (2004) Reduction of methemoglobin via electron transfer from photoreduced flavin: restoration of O_2-binding of concentrated hemoglobin solution coencapsulated in phospholipid vesicles. *Bioconjugate Chem. 15*, 1037–1045.

(55) Atoji, T., Aihara, M., Sakai, H., Tsuchida, E., and Takeoka, S. (2006) Hemoglobin vesicles containing methemoglobin and L-tyrosine to suppress methemoglobin formation *in vitro* and *in vivo*. *Bioconjugate Chem. 17*, 1241–1245.

(56) Sakai, H., Takeoka, S., Seino, Y., and Tsuchida, E. (1994) Suppression of methemoglobin formation by glutathione in a concentrated hemoglobin solution and in a Hb-vesicle. *Bull. Chem. Soc. Jpn. 67*, 1120–1125.

(57) Rameez, S., Alosta, H., and Palmer, A. F. (2008) Biocompatible and biodegradable polymersome encapsulated hemoglobin: a potential oxygen carrier. *Bioconjugate Chem. 19*, 1025–1032.

(58) Zhao, J., Liu, C. S., Yuan, Y., Tao, X. Y., Shan, X. Q., Sheng, Y., and Wu, F. (2007) Preparation of hemoglobin-loaded nano-sized particles with porous structure as oxygen carriers. *Biomaterials 28*, 1414–1422.

(59) Rudolph, A. S. (1988) The freeze-dried preservation of liposome encapsulated hemoglobin: a potential blood substitute. *Cryobiology 25*, 277–284.

(60) Rabinovici, R., Rudolph, A. S., Vernick, J., and Feuerstein, G. (1994) Lyophilized liposome encapsulated hemoglobin: evaluation of hemodynamic, biochemical, and hematologic responses. *Crit. Care Med. 22*, 480–485.

(61) Ringsdorf, H., Schlarb, B., and Venzmer, J. (1988) Molecular architecture and function of polymeric oriented systems - models for the study of organization, surface recognition, and dynamics of biomembranes. *Angew. Chem., Int. Ed. 27*, 113–158.

(62) Kato, A., Arakawa, M., and Kondo, T. (1984) Preparation and stability of liposome-type artificial red blood cells stabilized with carboxymethylchitin. *J. Microencapsul. 1*, 105–112.

(63) Mobed, M., Nishiya, T., and Chang, T. M. (1992) Preparation of carboxymethylchitin-incorporated submicron bilayer-lipid membrane artificial cells (liposomes) encapsulating hemoglobin. *Biomater. Artif. Cells Immobil. Biotechnol. 20*, 365–368.

(64) Li, S., Nickels, J., and Palmer, A. F. (2005) Liposome-encapsulated actin-hemoglobin (LEAcHb) artificial blood substitutes. *Biomaterials 26*, 3759–3769.

(65) Tsuchida, E., Hasegawa, E., Kimura, N., Hatashita, M., and Makino, C. (1992) Polymerization of unsaturated phospholipids as large unilamellar liposomes at low temperature. *Macromolecules 25*, 2007–212.

(66) Sakai, H., Takeoka, S., Yokohama, H., Nishide, H., and Tsuchida, E. (1992) Encapsulation of Hb into unsaturated lipid vesicles and gamma-ray polymerization. *Polym. Adv. Technol. 3*, 389–394.

(67) Akama, K., Awai, K., Yano, Y., Tokuyama, S., and Nakano, Y. (2000) In vitro and in vivo stability of polymerized mixed liposomes composed of 2,4-octadecadienoyl groups of phospholipids. *Polym. Adv. Technol 11*, 280–287.

(68) Sakai, H., Takeoka, S., Park, S. I., Kose, T., Nishide, H., Izumi, Y., Yoshizu, A., Kobayashi, K., and Tsuchida, E. (1997) Surface-modification of hemoglobin vesicles with poly(ethylene glycol) and effects on aggregation, viscosity, and blood flow during 90%-exchange transfusion in anesthetized rats. *Bioconjugate Chem. 8*, 23–30.

(69) Sakai, H., Tsai, A. G., Kerger, H., Park, S. I., Takeoka, S., Nishide, H., Tsuchida, E., and Intaglietta, M. (1998) Subcutaneous microvascular responses to hemodilution with red cell substitutes consisting of polyethylene glycol-modified vesicles encapsulating hemoglobin. *J. Biomed. Mater. Res. 40*, 66–78.

(70) Sakai, H., Okamoto, M.,; Ikeda E., Horinouchi H., Kobayashi K., and Tsuchida, E. (2008) Histopathological changes of rat brain after direct injection of hemoglobin vesicles (oxygen carriers) and neurological impact in an intracerebral hemorrhage model. *J. Biomed. Mater. Res., Part A* (in press).

(71) Sakai, H., Tomiyama, K., Sou, K., Takeoka, S., and Tsuchida, E. (2000) Poly(ethylene glycol)-conjugation and deoxygenation enable long-term preservation of hemoglobin vesicles as oxygen carriers in a liquid state. *Bioconjugate Chem. 11*, 425–432.

(72) Sou, K., Endo, T., Takeoka, S., and Tsuchida, E. (2000) Poly(ethylene glycol)-modification of the phospholipid vesicles by using the spontaneous incorporation of poly(ethylene glycol)-lipid into the vesicles. *Bioconjugate Chem. 11*, 372–379.

(73) Sato, T., Sakai, H., Sou, K., Buchner, R., and Tsuchida, E. (2007) Poly(ethylene glycol)-conjugated phospholipids in aqueous micellar solutions: hydration, static structure, and interparticle interactions. *J. Phys. Chem. B 111*, 1393–1401.

(74) Szebeni, J. (2005) Complement activation-related pseudoallergy: a new class of drug-induced acute immune toxicity. *Toxicology 216*, 106–121.

(75) Van de Velde, M., Wouters, P. F., Rolf, N., Van Aken, H., and Vandermeersch, E. (1998) Comparative hemodynamic effects of three different parenterally administered lipid emulsions in conscious dogs. *Crit. Care Med. 26*, 132–137.

(76) Vercellotti, G. M., Hammerschmidt, D. E., Craddock, P. R., and Jacob, H. S. (1982) Activation of plasma complement by perfluorocarbon artificial blood: probable mechanism of adverse pulmonary reactions in treated patients and rationale for corticosteroids prophylaxis. *Blood 59*, 1299–1304.

(77) Phillips, W. T., Klipper, R., Fresne, D., Rudolph, A. S., Javors, M., and Goins, B. (1997) Platelet reactivity with liposome-encapsulated hemoglobin in the rat. *Exp. Hematol. 25*, 1347–1356.

(78) Szebeni, J., Fontana, J. L., Wassef, N. M., Mongan, P. D., Morse, D. S., Dobbins, D. E., Stahl, G. L., Bunger, R., and Alving, C. R. (1999) Hemodynamic changes induced by liposomes and liposome-encapsulated hemoglobin in pigs: a model for pseudoallergic cardiopulmonary reactions to liposomes. Role of complement and inhibition by soluble CR1 and anti-C5a antibody. *Circulation 99*, 2302–2309.

(79) Izumi, Y., Sakai, H., Kose, T., Hamada, K., Takeoka, S., Yoshizu, A., Horinouchi, H., Kato, R., Nishide, H., Tsuchida, E., and Kobayashi, K. (1997) Evaluation of the capabilities of a hemoglobin vesicle as an artificial oxygen carrier in a rat exchange transfusion model. *ASAIO J. 43*, 289–297.

(80) Loughrey, H. C., Bally, M. B., Reinish, L. W., and Cullis, P. R. (1990) The binding of phosphatidylglycerol liposomes to rat platelets is mediated by complement. *Thromb. Haemost. 64*, 172–176.

(81) Chonn, A., Cullis, P. R., and Devine, D. V. (1991) The role of surface charge in the activation of the classical and alternative pathways of complement by liposomes. *J. Immunol. 146*, 4234–4241.

(82) Sou, K., and Tsuchida, E. (2008) Electrostatic interactions and complement activation on the surface of phospholipid vesicle containing acidic lipids: effect of the structure of acidic groups. *Biochim. Biophys. Acta - Biomembr. 1778*, 1035–1041.

(83) Abe, H., Azuma, H., Yamaguchi, M., Fujihara, M., Ikeda, H., Sakai, H., Takeoka, S., and Tsuchida, E. (2007) Effects of hemoglobin vesicles, a liposomal artificial oxygen carrier, on hematological responses, complement and anaphylactic reactions in rats. *Artif. Cells Blood Substit. Biotechnol. 35*, 157–172.

(84) Abe, H., Fujihara, M., Azuma, H., Ikeda, H., Ikebuchi, K., Takeoka, S., Tsuchida, E., and Harashima, H. (2006) Interaction of hemoglobin vesicles, a cellular-type artificial oxygen carrier, with human plasma: effects on coagulation, kallikrein-kinin, and complement systems. *Artif. Cells Blood Substit. Immobil. Biotechnol. 34*, 1–10.

(85) Wakamoto, S., Fujihara, M., Abe, H., Yamaguchi, M., Azuma, H., Ikeda, H., Takeoka, S., and Tsuchida, E. (2005) Effects of hemoglobin vesicles on resting and agonist-stimulated human platelets *in vitro*. *Artif. Cells Blood Substit. Immobil. Biotechnol. 33*, 101–111.

(86) Wakamoto, S., Fujihara, M., Abe, H., Sakai, H., Takeoka, S., Tsuchida, E., Ikeda, H., and Ikebuchi, K. (2001) Effects of poly(ethyleneglycol)-modified hemoglobin vesicles on agonist-induced platelet aggregation and RANTES release *in vitro*. *Artif. Cells Blood Substit. Immobil. Biotechnol. 29*, 191–201.

(87) Takeoka, S., Mori, K., Ohkawa, H., Sou, K., and Tsuchida, E. (2000) Synthesis and assembly of poly(ethylene glycol)-lipids with mono-, di-, and tetraacyl chains and a poly(ethylene glycol) chain of various molecular weights. *J. Am. Chem. Soc. 122*, 7927–7935.

(88) Okamura, Y., Maekawa, I., Teramura, Y., Maruyama, H., Handa, M., Ikeda, Y., and Takeoka, S. (2005) Hemostatic effects of phospholipid vesicles carrying fibrinogen gamma chain dodecapeptide *in vitro* and *in vivo*. *Bioconjugate Chem. 16*, 1589–1596.

(89) Ohkawa, H., Teramura, Y., Takeoka, S., and Tsuchida, E. (2000) Synthesis of multiacyl poly(ethylene glycol) for the conjugation of cytochrome c to phospholipid vesicle. *Bioconjugate Chem. 11*, 815–821.

(90) Sou, K., Goins, B., Takeoka, S., Tsuchida, E., and Phillips, W. T. (2007) Selective uptake of surface-modified phospholipid vesicles by bone marrow macrophages *in vivo*. *Biomaterials 28*, 2655–2666.

(91) Teramura, Y., and Iwata, H. (2008) Islets surface modification prevents blood-mediated inflammatory responses. *Bioconjugate Chem. 19*, 1389–1395.

(92) Obata, Y., Suzuki, D., and Takeoka, S. (2008) Evaluation of cationic assemblies constructed with amino acid based lipids for plasmid DNA delivery. *Bioconjugate Chem. 19*, 1055–1063.

(93) Sou, K., Inenaga, S., Takeoka, S., and Tsuchida, E. (2008) Loading of curcumin into macrophages using lipid-based nanoparticles. *Int. J. Pharm. 352*, 287–293.

(94) Sou, K., Klipper, R., Goins, B., Tsuchida, E., and Phillips, W. T. (2005) Circulation kinetics and organ distribution of Hb vesicles developed as a red blood cell substitute. *J. Pharmacol. Exp. Ther. 312*, 702–709.

(95) Bradley, A. J., Devine, D. V., Ansell, S. M., Janzen, J., and Brooks, D. E. (1998) Inhibition of liposome-induced complement activation by incorporated poly(ethylene glycol)-lipids. *Arch. Biochem. Biophys. 357*, 185–194.

(96) Hu, Q., and Liu, D. (1996) Co-existence of serum-dependent and serum-independent mechanisms for liposome clearance and involvement of non-Kupffer cells in liposome uptake by mouse liver. *Biochim. Biophys. Acta 1284*, 153–161.

(97) Shibuya-Fujiwara, N., Hirayama, F., Ogata, Y., Ikeda, H., and Ikebuchi, K. (2001) Phagocytosis *in vitro* of polyethylene glycol-modified liposome-encapsulated hemoglobin by human peripheral blood monocytes plus macrophages through scavenger receptors. *Life Sci. 70*, 291–300.

(98) Sakai, H., Horinouchi, H., Tomiyama, K., Ikeda, E., Takeoka, S., Kobayashi, K., and Tsuchida, E. (2001) Hemoglobin-vesicles as oxygen carriers: influence on phagocytic activity and histopathological changes in reticuloendothelial system. *Am. J. Pathol. 159*, 1079–1088.

(99) Sakai, H., Horinouchi, H., Masada, Y., Takeoka, S., Kobayashi, K., and Tsuchida, E. (2004) Metabolism of hemoglobin-vesicles (artificial oxygen carriers) and their influence on organ functions in a rat model. *Biomaterials 25*, 4317–4325.

(100) Sakai, H., Masada, Y., Horinouchi, H., Ikeda, E., Sou, K., Takeoka, S., Suematsu, M., Takaori, M., Kobayashi, K., and Tsuchida, E. (2004) Physiologic capacity of reticuloendothelial system for degradation of hemoglobin-vesicles (artificial oxygen carriers) after massive intravenous doses by daily repeated infusions for 14 days. *J. Pharmacol. Exp. Ther. 311*, 874–884.

(101) Sakai, H., Horinouchi, H., Yamamoto, M., Ikeda, E., Takeoka, S., Takaori, M., Tsuchida, E., and Kobayashi, K. (2006) Acute 40% exchange-transfusion with hemoglobin-vesicles (HbV) suspended in recombinant human serum albumin solution: degradation of HbV and erythropoiesis in a rat spleen for 2 weeks. *Transfusion 46*, 339–347.

(102) Sakai, H., Seishi, Y., Obata, Y., Takeoka, S., Horinouichi, H., Tsuchida, E., and Kobayashi, K. (2009) Fluid resuscitation with artificial oxygen carriers in hemorrhaged rats: Profiles of hemoglobin-vesicle degradation and hematopoiesis for 14 days. *Shock 31*, 192–200.

(103) Yamaoka, T., Tabata, Y., and Ikada, Y. (1994) Distribution and tissue uptake of poly(ethylene glycol) with different molecular weights after intravenous administration to mice. *J. Pharm. Sci. 83*, 601–606.

(104) Ohki, N., Kimura, T., and Ogata, Y. (1998) The reduction of methemoglobin in Neo Red Cell. *Artif. Cells Blood Substit. Immobil. Biotechnol. 26*, 477–485.

(105) Sakai, H., Tsai, A. G., Rohlfs, R. J., Hara, H., Takeoka, S., Tsuchida, E., and Intaglietta, M. (1999) Microvascular responses to hemodilution with Hb vesicles as red cell substitutes: Influences of O_2 affinity. *Am. J. Physiol. Heart Circ. Physiol. 276*, H553–H562.

(106) Wang, L., Morizawa, K., Tokuyama, S., Satoh, T., and Tsuchida, E. (1992) Modulation of oxygen-carrying capacity of artificial red cells (ARC). *Polym. Adv. Technol. 4*, 8–11.

(107) Cabrales, P., Sakai, H., Tsai, A. G., Takeoka, S., Tsuchida, E., and Intaglietta, M. (2005) Oxygen transport by low and normal oxygen affinity hemoglobin vesicles in extreme hemodilution. *Am. J. Physiol. Heart Circ. Physiol. 288*, H1885–H1892.

(108) Izumi, Y., Sakai, H., Hamada, K., Takeoka, S., Yamahata, T., Kato, R., Nishide, H., Tsuchida, E., and Kobayashi, K. (1996) Physiologic responses to exchange transfusion with hemoglobin vesicles as an artificial oxygen carrier in anesthetized rats: changes in mean arterial pressure and renal cortical oxygen tension. *Crit. Care Med. 24*, 1869–1873.

(109) Sakai, H., Takeoka, S., Wettstein, R., Tsai, A. G., Intaglietta, M., and Tsuchida, E. (2002) Systemic and Microvascular responses to the hemorrhagic shock and resuscitation with Hb vesicles. *Am. J. Physiol. Heart Circ. Physiol. 283*, H1191−H1199.

(110) Sakai, H., Masada, Y., Horinouchi, H., Yamamoto, M., Ikeda, E., Takeoka, S., Kobayashi, K., and Tsuchida, E. (2004) Hemoglobin vesicles suspended in recombinant human serum albumin for resuscitation from hemorrhagic shock in anesthetized rats. *Crit. Care Med. 32*, 539–545.

(111) Yoshizu, A., Izumi, Y., Park, S. I., Sakai, H., Takeoka, S., Horinouchi, H., Ikeda, E., Tsuchida, E., and Kobayashi, K. (2004) Hemorrhagic shock resuscitation with an artificial oxygen carrier hemoglobin vesicle (HbV) maintains intestinal perfusion and suppresses the increase in plasma necrosis factor alpha (TNFα). *ASAIO J. 50*, 458–463.

(112) Terajima, K., Tsueshita, T., Sakamoto, A., and Ogawa, R. (2006) Fluid resuscitation with hemoglobin vesicles in a rabbit model of acute hemorrhagic shock. *Shock 25*, 184–189.

(113) Yamazaki, M., Aeba, R., Yozu, R., and Kobayashi, K. (2006) Use of hemoglobin vesicles during cardiopulmonary bypass priming prevents neurocognitive decline in rats. *Circulation 114* (1 Suppl), I220−I225.

(114) Tsai, A. G., Vandegriff, K. D., Intaglietta, M., and Winslow, R. M. (2003) Targeted O_2 delivery by low-P_{50} hemoglobin: a new basis for O_2 therapeutics. *Am. J. Physiol. Heart Circ. Physiol. 285*, H1411−H1419.

(115) Plock, J. A., Tromp, A. E., Contaldo, C., Spanholtz, T., Sinovcic, D., Sakai, H., Tsuchida, E., Leunig, M., Banic, A., and Erni, D. (2007) Hemoglobin vesicles reduce hypoxia-related inflammation in critically ischemic hamster flap tissue. *Crit. Care Med. 35*, 899–905.

(116) Nolte, D., Pickelmann, S., Lang, M., Keipert, P., and Messmer, K. (2000) Compatibility of different colloid plasma expanders with perflubron emulsion: an intravital microscopic study in the hamster. *Anesthesiology 93*, 1261–1270.

(117) Jouan-Hureaux, V., Audonnet-Blaise, S., Lacatusu, D., Krafft, M. P., Dewachter, P., Cauchois, G., Stoltz, J. F., Longrois, D., and Menu, P. (2006) Effects of a new perfluorocarbon emulsion on human plasma and whole-blood viscosity in the presence of albumin, hydroxyethyl starch, or modified fluid gelatin: an in vitro rheologic approach. *Transfusion 46*, 1892–1898.

(118) Vandegriff, K. D., McCarthy, M., Rohlfs, R. J., and Winslow, R. M. (1997) Colloid osmotic properties of modified hemoglobins: chemically cross-linked versus polyethylene glycol surface-conjugated. *Biophys. Chem. 69*, 23–30.

(119) Kobayashi, K. (2006) Summary of recombinant human serum albumin development. *Biologicals 34*, 55–59.

(120) Meyuhas, D., Nir, S., and Lichtenberg, D. (1996) Aggregation of phospholipid vesicles by water-soluble polymers. *Biophys. J. 71*, 2602–2612.

(121) Neu, B., and Meiselman, H. J. (2002) Depletion-mediated red blood cell aggregation in polymer solutions. *Biophys. J. 83*, 2482–2490.

(122) Sakai, H., Sato, A., Takeoka, S., and Tsuchida, E. (2007) Rheological property of hemoglobin vesicles (artificial oxygen carriers) suspended in a series of plasma substitute aqueous solutions. *Langmuir 23*, 8121–8128.

(123) Tsai, A. G., Friesenecker, B., McCarthy, M., Sakai, H., and Intaglietta, M. (1998) Plasma viscosity regulates capillary perfusion during extreme hemodilution in hamster skinfold model. *Am. J. Physiol. Heart Circ. Physiol. 275*, H2170−H2180.

(124) Intaglietta, M., Cabrales, P., and Tsai, A. G. (2006) Microvascular perspective of oxygen-carrying and -noncarrying blood substitutes. *Annu. Rev. Biomed. Eng. 8*, 289–321.

(125) Rebel, A., Ulatowski, J. A., Kwansa, H., Bucci, E., and Koehler, R. C. (2003) Cerebrovascular response to decreased hematocrit: effect of cell-free hemoglobin, plasma viscosity, and CO_2. *Am. J. Physiol. Heart Circ. Physiol. 285*, H1600−H1608.

(126) Dimino, M. L., and Palmer, A. F. (2007) High O_2 affinity hemoglobin-based oxygen carriers synthesized via polymerization of hemoglobin with ring-opened 2-chloroethyl-β-D-fructopyranoside and 1-o-octyl-β-D-glucopyranoside. *Biotechnol. Bioeng. 97*, 462–472.

(127) Plock, J. A., Contaldo, C., Sakai, H., Tsuchida, E., Leunig, M., Banic, A., Menger, M. D., and Erni, D. (2005) Is the Hb in Hb vesicles infused for isovolemic hemodilution necessary to improve oxygenation in critically ischemic hamster skin? *Am. J. Physiol. Heart Circ. Physiol. 289*, H2624−H2631.

(128) Contaldo, C., Plock, J., Sakai, H., Takeoka, S., Tsuchida, E., Leunig, M., Banic, A., and Erni, D. (2005) New generation of hemoglobin-based oxygen carriers evaluated for oxygenation of critically ischemic hamster flap tissue. *Crit. Care Med. 33*, 806–812.

(129) Verdu, E. F., Bercik, P., Huang, X. X., Lu, J., Al-Mutawaly, N., Sakai, H., Tompkins, T. A., Croitoru, K., Tsuchida, E., Perdue, M., and Collins, S. M. (2008) The role of luminal factors in the recovery of gastric function and behavioral changes after chronic *Helicobacter pylori* infection. *Am. J. Physiol. Gastrointest. Liver Physiol. 295*, G664−G670.

(130) Komatsu, H., Furuya, T., Sato, N., Ohta, K., Matsuura, A., Ohmura, T., Takagi, S., Matsuura, M., Yamashita, M., Itoda, M., Itoh, J., Horinouchi, H., and Kobayashi, K. (2007) Effect of hemoglobin vesicle, a cellular-type artificial oxygen carrier, on middle cerebral artery occlusion- and arachidonic acid-induced stroke models in rats. *Neurosci. Lett. 421*, 121–125.

(131) Yamamoto, M., Izumi, Y., Horinouchi, H., Teramura, Y., Sakai, H., Kohno, M., Watanabe, M., Kawamura, M., Adachi, T., Ikeda, E., Takeoka, S., Tsuchida, E., Kobayashi, K. (2009) Systemic administration of hemoglobin vesicle elevates tumor tissue oxygen tension and modifies tumor response to irradiation. *J. Surg. Res.* doi:10.1016/j.jss. 2007 12 770.

(132) Sakai, H., Horinouchi, H., Tsuchida, E., Kobayashi, K. (2008) Hemoglobin-vesicles and red blood cells as carriers of carbon monoxide prior to oxygen for resuscitation after hemorrhagic shock in a rat model. *Shock.* doi:10 1097/SHK.0b013e318189017a.

(133) Peters, T. (1996) *All about Albumin*: Biochemistry, Genetics and Medical Applications, Academic Press, San Diego.

(134) He, X. M., and Carter, D. C. (1992) Atomic structure and chemistry of human serum albumin. *Nature 358*, 209–215.

(135) Carter, D. C., and Ho, J. X. (1994) Structure of serum albumin. *Adv. Protein Chem. 45*, 153–203.

(136) Curry, S., Madelkow, H., Brick, P., and Franks, N. P. (1998) Crystal structure of human serum albumin complexed with fatty acid reveals an asymmetric distribution of binding sites. *Nat. Struct. Biol. 5*, 827–835.

(137) Bhattacharya, A. A., Grune, T., and Curry, S. (2000) Crystal structures of human serum albumin complexed with monounsaturated and polyunsaturated fatty acids. *J. Mol. Biol. 303*, 721–732.

(138) Ghuman, J., Zunszain, P. A., Petitpas, I., Bhattacharya, A. A., Otagiri, M., and Curry, S. (2007) Structural basis of the drug-binding specificity of humans serum albumin. *J. Mol. Biol. 353*, 38–52.

(139) Tsuchida, E., Komatsu, T., Matsukawa, Y., Hamamatsu, K., and Wu, J. (1999) Human serum albumin incorporating tetrakis(o-pivalamido)phenyl porphinatoiron(II) derivative as a totally synthetic O_2-carrying hemoprotein. *Bioconjugate Chem. 10*, 797–802.

(140) Komatsu, T., Hamamatsu, K., Wu, J., and Tsuchida, E. (1999) Physicochemical properties and O_2-coordination structure of human serum albumin incorporating tetrakis-(o-pivalamido) phenylporphyrinatoiron(II) derivatives. *Bioconjugate Chem. 10*, 82–86.

(141) Tsuchida, E., Komatsu, T., Yanagimoto, T., and Sakai, H. (2003) Preservation stability and *in vivo* administration of albumin-heme hybrid solution as an entirely synthetic O_2-carrier. *Polym. Adv. Technol. 13*, 848–850.

(142) Huang, Y., Komatsu, T., Nakagawa, A., Tsuchida, E., and Kobayashi, S. (2003) Compatibility *in vitro* of albumin-heme

(O_2 carrier) with blood cell components. *J. Biomed. Mater. Res. 66A*, 292–297.

(143) Komatsu, T., Huang, Y., Wakamoto, S., Abe, H., Fujihara, M., Azuma, H., Ikeda, H., Yamamoto, H., Horinouchi, H., and Kobayashi, K. (2007) Influence of O_2-carrying plasma hemoprotein "albumin-heme" on complement system and platelet activation *in vitro* and physiological responses to exchange transfusion. *J. Biomed. Mater. Res. 81A*, 821–826.

(144) Tsuchida, E., Nakagawa, A., and Komatsu, T. (2003) Coordination structure of active site in synthetic hemoprotein (albumin-heme) with dioxygen and carbon monoxide. *Macromol. Symp. 195*, 275–280.

(145) Komatsu, T., Matsukawa, Y., and Tsuchida, E. (2000) Nitrosyl iron(II) complex of *meso*-tetrakis(α,α,α,α-o-pivalamidophenyl)porphyrin with a covalently linked 2-methylimidazolylalkyl group. *Chem. Lett.* 1060–1061.

(146) Komatsu, T., Matsukawa, Y., and Tsuchida, E. (2001) Reaction of nitric oxide with synthetic hemoprotein, human serum albumin incorporating tetraphenylporphinatoiron(II) derivatives. *Bioconjugate Chem. 12*, 71–75.

(147) Collman, J. P., Brauman, J. I., Iverson, B. L., Sessler, J. L., Morris, R. M., and Gibson, Q. H. (1983) O_2 and CO binding to iron(II) porphyrins: A comparison of the "picket fence" and "pocket" porphyrins. *J. Am. Chem. Soc. 105*, 3052–3064.

(148) Traylor, T. G., Tsuchiya, S., Campbell, D., Mitchell, M., Stynes, D., and Koga, N. (1985) Anthracene-heme cyclophanes. Sterice in CO, O_2 and RNC binding. *J. Am. Chem. Soc. 107*, 604–614.

(149) Komatsu, T., Matsukawa, Y., and Tsuchida, E. (2000) Kinetics of CO and O_2 binding to human serum albumin-heme hybrid. *Bioconjugate Chem. 11*, 772–776.

(150) Komatsu, T., Matsukawa, Y., and Tsuchida, E. (2002) Effect of heme structure on O_2-binding properties of human serum albumin-heme hybrids: intramolecular histidine coordination provides a stable O_2-adduct complex. *Bioconjugate Chem 13*, 397–402.

(151) Nakagawa, A., Komatsu, T., Iizuka, M., and Tsuchida, E. (2008) O_2 binding to human serum albumin incorporating iron porphyrin with a covalently linked methyl-L-histidine isomer. *Bioconjugate Chem. 19*, 581–584.

(152) Nakagawa, A., Komatsu, T., and Tsuchida, E. (2007) meso-Tetrakis(α,α,α,α-o-amidophenyl) porphinatoiron(II) bearing a proximal histidyl group at the β-pyrrolic position via an acyl bond: synthesis and O_2 coordination in aqueous media. *Chem. Lett. 36*, 640–641.

(153) Komatsu, T., Okada, T., Moritake, M., and Tsuchida, E. (2001) O_2-binding properties of double-sided porphinatoiron(II)s with polar substituents and their human serum albumin hybrids. *Bull. Chem. Soc. Jpn. 74*, 1695–1702.

(154) Nakagawa, A., Komatsu, T., Iizuka, M., and Tsuchida, E. (2006) Human serum albumin hybrid incorporating tailed porphyrinatoiron(II) in the α,α,α,β-conformer as an O_2-binding site. *Bioconjugate Chem. 17*, 146–151.

(155) Nakagawa, A., Komatsu, T., Ohmichi, N., and Tsuchida, E. (2003) Synthetic dioxygen-carrying hemoprotein. human serum albumin including iron(II) complex of protoporphyrin IX with an axially coordinated histidylglycyl-propionate. *Chem. Lett. 32*, 504–505.

(156) Nakagawa, A., Komatsu, T., Ohmichi, N., and Tsuchida, E. (2004) Synthesis of protoheme IX derivatives with a covalently linked proximal base and their human serum albumin hybrids as artificial hemoprotein. *Org. Biomol. Chem. 2*, 3108–3112.

(157) Wang, R.-M., Komatsu, T., Nakagawa, A., and Tsuchida, E. (2005) Human serum albumin bearing covalently attached iron(II) porphyrins as O_2-coordination sites. *Bioconjugate Chem. 16*, 23–26.

(158) Harris, J. M. (1992) *Poly(ethylene glycol) Chemistry: Biotechnical and Biomedical Applications* (Harris, J. M., Ed.) Plenum Press, New York.

(159) Veronese, F. M., and Harris, J. M. (2002) Introduction and overview of peptide and protein PEGylation. *Adv. Drug Delivery Rev. 54*, 453–456.

(160) Roberts, M. J., Bentley, M. D., and Harris, J. M. (2002) Chemistry for peptide and protein PEGylation. *Adv. Drug Delivery Rev. 54*, 459–476.

(161) Veronese, F. M. (2001) Peptide and protein PEGylation: a review of problems and solutions. *Biomaterials 22*, 405–417.

(162) Nucci, M. L., Shorr, R., and Abuchowski, A. (1991) The therapeutic value of poly(ethylene glycol) modified proteins. *Adv. Drug Delivery Rev. 6*, 133–151.

(163) Kawahara, N. Y., and Ohno, H. (1997) Induced thermostability of poly(ethylene oxide)-modified hemoglobin in glycols. *Bioconjugate Chem. 8*, 643–648.

(164) Huang, Y., Komatsu, T., Wang, R.-M., Nakagawa, A., and Tsuchida, E. (2006) Poly(ethylene glycol)-conjugated human serum albumin including iron porphyrins: surface modification improves the O_2-transporting ability. *Bioconjugate Chem. 17*, 393–398.

(165) Cabrales P., Tsai, A. G., Intaglietta, M. (2004) Microvascular pressure and functional capillary density in extreme hemodilution with low- and high-viscosity dextran and a low-viscosity Hb-based O_2 carrier. *Am. J. Physiol. Heart Circ. Physiol. 287*, H363−H373.

(166) Martini, J., Cabrales, P., K, A., Acharya, S. A., Intaglietta, M., Tsai, A. G. (2008) Survival time in severe hemorrhagic shock after perioperative hemodilution is longer with PEG-conjugated human serum albumin than HES 130/0.4: a microvasucular perspective. *Crit. Care 12*, R54.

(167) Sugawara, Y., and Shikama, K. (1980) Autoxidation of native oxymyoglobin. *Eur. J. Biochem. 110*, 241–246.

(168) Tsuchida, E., Komatsu, T., Hamamatsu, K., Matsukawa, Y., Tajima, A., Yoshizu, A., Izumi, Y., and Kobayashi, K. (2000) Exchange transfusion with albumin-heme as an artificial O_2-infusion into anesthetized rats: physiological responses, O_2-delivery, and reduction of the oxidized hemin sites by red blood cells. *Bioconjugate Chem. 11*, 46–50.

(169) Huang, Y., Komatsu, T., Yamamoto, H., Horinouchi, H., Kobayashi, K., and Tsuchida, E. (2006) PEGylated albumin-heme as an oxygen-carrying plasma expander: exchange transfusion into acute anemia rat model. *Biomaterials 27*, 4477–4483.

(170) Tsuchida, E., Komatsu, T., Matsukawa, Y., Nakagawa, A., Sakai, H., Kobayashi, K., and Suematsu, M. (2003) Human serum albumin incorporating synthetic heme: red blood cell substitute without hypertension by nitric oxide scavenging. *J. Biomed. Mater. Res. 64A*, 257–261.

(171) Nakagawa, A., Komatsu, T., Huang, H., Lu, G., and Tsuchida, E. (2007) O_2-binding albumin thin films: solid membranes of poly(ethylene glycol)-conjugated human serum albumin incorporating iron porphyrin. *Bioconjugate Chem. 18*, 1673–1677.

(172) Goa, K. L., and Benfield, P. (1994) Hyaluronic-acid - a review of its pharmacology and use as a surgical and in ophthalmology, and its therapeutic potential in joint disease and wound-healing. *Drugs 47*, 536–566.

(173) Adams, P. A., and Berman, M. C. (1980) Kinetics and mechanism of the interaction between human serum albumin and monomeric haemin. *Biochem. J. 191*, 95–102.

(174) Zunszain, P. A., Ghuman, J., Komatsu, T., Tsuchida, E., and Curry, S. (2003) Crystal structural analysis of human serum albumin complexed with hemin and fatty acid. *BMC Struct. Biol. 3*, 6.

(175) Wardell, M., Wang, Z., Ho, J. X., Robert, J., Ruker, F., Ruble, J., and Carter, D. C. (2002) The atomic structure of human methemalbumin at 1.9 Å. *Biochem. Biophys. Res. Commun. 291*, 813–819.

(176) Komatsu, T., Ohmichi, N., Zunszain, P. A., Curry, S., and Tsuchida, E. (2004) Dioxygenation of human serum albumin having a prosthetic-heme group in a tailor-made heme pocket. *J. Am. Chem. Soc. 126*, 14304–14305.

(177) Komatsu, T., Ohmichi, N., Nakagawa, A., Zunszain, P. A., Curry, S., and Tsuchida, E. (2005) O_2 and CO binding properties of artificial hemoproteins formed by complexing iron protoporphyrin IX with human serum albumin mutants. *J. Am. Chem. Soc. 127*, 15933–15942.

(178) Vickery, L., Nozawa, T., and Sauer, K. (1976) Magnetic circular dichroism studies of myoglobin complexes. Correlation

with-heme spin state and axial ligation. *J. Am. Chem. Soc. 98*, 343–350.

(179) Antonini, E., and Brunori, M. *Hemoglobin and Myoglobin in Their Reactions with Ligands*, p 18, North-Holland Publishers, Amsterdam.

(180) Rohlfs, R., Mathews, A. J., Carver, T. E., Olson, J. S., Springer, B. A., Egeberg, K. D., and Sligar, S. G. (1990) The effects of amino acid substitution at position E7 (residue 64) on the kinetics of ligand binding to sperm whale myoglobin. *J. Biol. Chem. 265*, 3168–3176.

(181) Imai, K., Morimoto, H., Kotani, M., Watari, H., Hirata, W., and Kuroda, M. (1970) Studies of the function of abnormal hemoglobins I. An improved method for automatic measurement of the oxygen equilibrium curve of hemoglobin. *Biochim. Biphys. Acta 200*, 189–197.

(182) Vandegriff, K. D., Young, M. A., Lohman, J., Bellelli, A., Samaja, M., Malavalli, A., and Winslow, R. M. (2008) CO-MP4, a polyethylene glycol-conjugated haemoglobin derivative and carbon monoxide carrier that reduces myocardial infarct size in rats. *Br. J. Pharmacol. 154*, 1649–1561.

(183) Creighton, T. E. (1992) *Proteins: Structures and Molecular Properties*, p 242, W. H. Freeman and Co., New York.

(184) Chu, M. M. L., Castro, C. E., and Hathaway, G. M. (1978) Oxidation of low-spin iron(II) porphyrins by molecular oxygen. An outer sphere mechanism. *Biochemistry 17*, 481–486.

(185) Tsuchida, E., Nishide, H., Sato, Y., and Kaneda, M. (1982) The preparation of protoheme mono-N-[5-(2-methyl-1-imidazolyl)pentyl]amide and its oxygenation. *Bull. Chem. Soc. Jpn. 55*, 1890–1895.

(186) Uno, T., Sakamoto, R., and Tomisugi, Y. (2003) Inversion of axial coordination in myoglobin to create a "proximal" ligand binding pocket. *Biochemistry 42*, 10191–10199.

(187) Springer, B. A., Sligar, S. G., Olson, J. S., and Philips, G. N. (1994) Mechanisms of a ligand recognition in myoglobin. *Chem. Rev. 94*, 699–714.

(188) Komatsu, T., Nakagawa, A., Zunszain, P. A., Curry, S., and Tsuchida, E. (2007) Genetic engineering of the heme pocket in human serum albumin: modulation of O_2 binding of iron protoporphyrin IX by variation of distal amino acids. *J. Am. Chem. Soc. 129*, 11286–11295.

BC800431D

O_2 Binding Properties of Human Serum Albumin Quadruple Mutant Complexed Iron Protoporphyrin IX with Axial His-186 Coordination

Akito Nakagawa,[1] Teruyuki Komatsu,*[1,2] Stephen Curry,[3] and Eishun Tsuchida[1]
[1]*Research Institute for Science and Engineering, Waseda University, 3-4-1 Okubo, Shinjuku-ku, Tokyo 169-8555*
[2]*PRESTO, Japan Science and Technology Agency (JST), 4-1-8 Honcho, Kawaguchi 332-0012*
[3]*Biophysics Section, Blackett Laboratory, Imperial College London, Exhibition Road, London SW7 2AZ, U.K.*

(Received May 18, 2009; CL-090494; E-mail: teruyuki@waseda.jp)

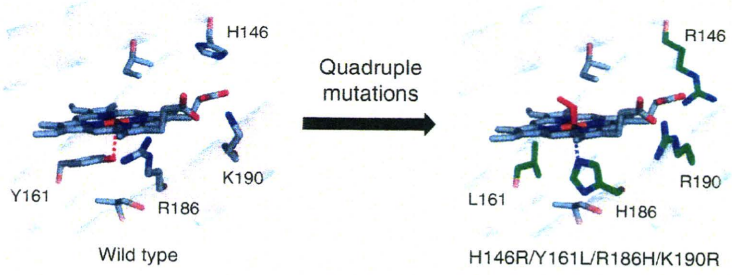

REPRINTED FROM

Chemistry Letters

Vol.38 No.8 2009 p.776–777
CMLTAG
August 5, 2009

The Chemical Society of Japan

Published on the web (Advance View) June 27, 2009; doi:10.1246/cl.2009.776

O_2 Binding Properties of Human Serum Albumin Quadruple Mutant Complexed Iron Protoporphyrin IX with Axial His-186 Coordination

Akito Nakagawa,[1] Teruyuki Komatsu,*[1,2] Stephen Curry,[3] and Eishun Tsuchida[1]
[1]*Research Institute for Science and Engineering, Waseda University, 3-4-1 Okubo, Shinjuku-ku, Tokyo 169-8555*
[2]*PRESTO, Japan Science and Technology Agency (JST), 4-1-8 Honcho, Kawaguchi 332-0012*
[3]*Biophysics Section, Blackett Laboratory, Imperial College London, Exhibition Road, London SW7 2AZ, U.K.*

(Received May 18, 2009; CL-090494; E-mail: teruyuki@waseda.jp)

The O_2 binding properties of complexes of iron(II) protoporphyrin IX with quadruple mutants of recombinant human serum albumin (rHSA) that provide axial His-186 coordination have been characterized; their O_2 binding parameters were similar to those of analogues having proximal His-185 and of human red blood cells.

In our bloodstream, iron(III) protoporphyrin IX (hemin) dissociated from methemoglobin (metHb) is captured by human serum albumin (HSA) and transported to liver cells for catabolism. Crystal structure analysis of this naturally occurring hemoprotein revealed that hemin is bound within a narrow D-shaped cavity in subdomain IB of HSA with a weak axial coordination by Tyr-161 and electrostatic interactions between the porphyrin propionate side-chains and three basic amino acid residues (Arg-114, His-146, and Lys-190) (Figure 1).[1,2] The axial phenolate ligation by Tyr-161 of HSA keeps the hemin group physiologically silent. In fact, the reduced ferrous HSA–heme is immediately oxidized by O_2.[3] We previously demonstrated that a pair of site-specific mutations in subdomain IB of HSA conferred O_2 binding capability on the heme: (i) introduction of a proximal His at Leu-185 position and (ii) substitution of Tyr-161 with noncoordinating Leu.[4a,4b] The resulting artificial hemoprotein can reversibly bind O_2 in much the same way as Hb and myoglobin (Mb). The albumin-based O_2 carrier has attracted medical interest because of its potential acting as a red blood cell (RBC) substitute. Interestingly, the proximal His introduced into the opposite side of the porphyrin plane (Ile-142 position) also allows O_2 binding to the heme.[4] These results suggest that there may be other sites where the proximal His can be inserted in the coordination sphere of the central iron. Our modeling and experimental results showed that Arg-186 is the third candidate because rHSA(I142H/Y161L/R186H)–heme formed a bishistidyl low-spin hemochrome.[4c] Furthermore, we have recently found that replacing His-146 and Lys-190 at the entrance of the heme pocket with Arg (H146R, K190R) resolved the structural heterogeneity of the two orientations of the porphyrin plane and afforded a single O_2 binding affinity.[4d]

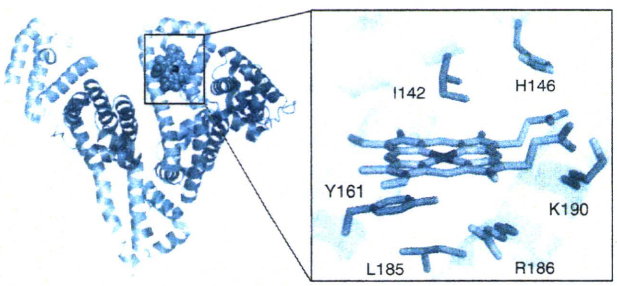

rHSA	Position				
	146	161	185	186	190
Wild type (wt)	His	Tyr	Leu	Arg	Lys
H146R/Y161G/R186H/K190R (1G)	**Arg**	**Gly**	Leu	**His**	**Arg**
H146R/Y161L/R186H/K190R (1L)	**Arg**	**Leu**	Leu	**His**	**Arg**
H146R/Y161G/L185H/K190R (2G)	**Arg**	**Gly**	**His**	Arg	**Arg**
H146R/Y161L/L185H/K190R (2L)	**Arg**	**Leu**	**His**	Arg	**Arg**

Figure 1. Structure of the heme pocket in the rHSA(wt)–hemin complex (PDB ID: 1O9X from ref 2).[5] Positions of the amino acids where site-specific mutations were introduced and abbreviations of the mutants are shown in the table. Structural models of the four rHSA(quadruple mutant)–heme complexes are demonstrated in Figure S1.[5,6]

In this study, we generated new rHSA(quadruple mutant)–heme complexes involving axial His-186 coordination and kinetically characterized their O_2 binding properties. The steric effect of the neighboring amino acid at the 161 position to the O_2 binding parameters is also investigated.

We designed rHSA quadruple mutants; rHSA(H146R/Y161G/R186H/K190R) [rHSA**1**G], rHSA(H146R/Y161L/R186H/K190R) [rHSA**1**L], rHSA(H146R/Y161G/L185H/K190R) [rHSA**2**G], and rHSA(H146R/Y161L/L185H/K190R) [rHSA**2**L] (Figure 1). Site-specific mutations were introduced into the HSA coding region in a plasmid vector (pHIL-D2 HSA) using the QuikChange (Stratagene) mutagenesis kit. All mutations were confirmed by DNA sequencing. The proteins were expressed in the yeast species *Pichia pastoris*. The corresponding ferric rHSA–hemin complexes were prepared according to our previously reported procedures.[4]

UV–vis absorption spectra of the four rHSA(quadruple mutant)–hemin complexes were essentially identical regarding their general features (Figure 2, Table S1).[6] They were easily reduced to the ferrous complexes by adding a small molar excess of aqueous $Na_2S_2O_4$ under an N_2 atmosphere (Figure S1).[6] A broad absorption band (λ = 557–559 nm) in the visible region was similar to that observed for deoxy Mb, indicating the formation of a five-N-coordinate high-spin ferrous complex.[7,8] Upon exposure of the rHSA–heme solution to O_2, the UV–vis absorption changed to that of the O_2 adduct complex (Figure 2).[4,7,8] After flowing CO gas, these hemoproteins produced stable carbonyl complexes. It can be concluded that the histidyl group at position 186 acts as a proximal base for dioxygenation of the prosthetic heme group. In contrast, rHSA(single mutant)–heme [rHSA(L185H)–heme and rHSA(R186H)–heme] could not bind O_2. In these complexes, Tyr-161 appears to coordinate to the central ferrous ion of the heme in competition with His-186 or His-185.

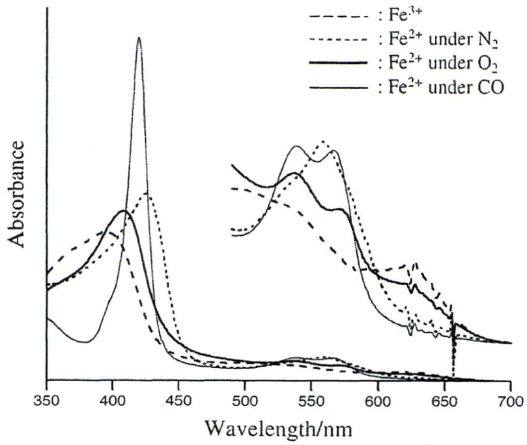

Figure 2. UV–vis. absorption spectral changes of rHSA1L–heme in 50 mM potassium phosphate buffered solution (pH 7.0) at 22 °C.

To determine the association and dissociation rate constants (k_{on} and k_{off}) for O_2 binding to rHSA(quadruple mutant)–heme, laser flash photolysis experiments were carried out.[4b] The O_2 recombination to the heme after the laser pulse irradiation occurs according to eq 1.

$$\text{Heme} + O_2 \underset{k_{off}}{\overset{k_{on}}{\rightleftarrows}} \text{Heme-}O_2 \qquad (1)$$

$$[P_{1/2} = K^{-1} = (k_{on}/k_{off})^{-1}]$$

The time dependences of the absorbance decays accompanying the O_2 and CO recombinations to rHSA(quadruple mutant)–heme complexes were clearly monophasic (Figure S2).[6] This can be attributed to a uniform heme orientation in the subdomain IB by introduction of Arg into the His-146 and Lys-190 positions.[4] As a result, each hemoprotein showed a single O_2 binding affinity (Table 1). It is noteworthy that all the rHSA(quadruple mutant)–heme complexes exhibited similar O_2 binding parameters independent of the position of the axial base (His-185 or His-186) and the size of the hydrophobic amino acid residue at 161 (Gly or Leu). We had postulated that the small Gly-161 would provide greater room for the proximal His-186 (or His-185), thereby loosening the spatially confined axial ligation. In general, such fluctuation decreases the k_{off} value and enhances the O_2 binding.[4b,4c] However, this was not observed in dioxygenation of rHSA1G–heme and rHSA2G–heme. The O_2 binding affinities ($P_{1/2}$) of the rHSA(quadruple mutant)–heme complexes (5–8 Torr) are very close to that of the human RBC ($P_{1/2}$ = 8 Torr) and, therefore, well adapted for O_2 transport in the circulatory system.

In conclusion, we have prepared rHSA(quadruple mutant)–heme complexes, in which (i) the proximal His was introduced at position 186 (or 185), (ii) Tyr-161 was substituted with Gly or Leu, and (iii) His-146 and Lys-190 at the heme pocket entrance were replaced with Arg. These artificial hemoproteins formed O_2 adduct complexes with a similar O_2 binding affinity. On the basis of our systematic investigations on rHSA–heme,[4] we conclude that the favorable positions for proximal His insertion are 142, 185, and 186; in all cases Tyr-161 must be replaced with noncoordinating amino acid (e.g., Gly, Leu, Phe, though Ala, Val, or Ile may also be tolerated). This structural flexibility of the heme pocket architecture in HSA has enabled the creation not only of an artificial O_2 carrier using the most abundant plasma protein but may also allow engineering of various hemoprotein enzymes.

Table 1. O_2 binding parameters of rHSA(quadruple mutant)–heme in 50 mM potassium phosphate buffered solution (pH 7.0) at 22 °C

Hemoproteins	k_{on} /μM^{-1} s^{-1}	k_{off} /ms^{-1}	$P_{1/2}$ /Torr
rHSA1G–heme	39	0.36	6
rHSA1L–heme	67	0.54	5
rHSA2G–heme	36	0.46	8
rHSA2L–heme[a]	42	0.41	6
Hbα (R-state)	33[b]	0.013[c]	0.24
Mb[d]	14	0.012	0.51
RBC[e]			8

[a]Ref 4d. [b]In 0.1 M phosphate buffer (pH 7.0, 21.5 °C), ref 9. [c]In 10 mM phosphate buffer (pH 7.0, 20 °C), ref 10. [d]In 0.1 M phosphate buffer (pH 7.0, 20 °C), ref 11. [e]Human RBC suspension, in isotonic buffer (pH 7.4, 20 °C), ref 12.

This work was partially supported by Grant-in-Aid for Scientific Research (No. 20750142 and No. 20350058) from JSPS, PRESTO from JST, and Health Science Research Grants from MHLW Japan.

References and Notes

1 M. Wardell, Z. Wang, J. X. Ho, J. Robert, F. Ruker, J. Ruble, D. C. Carter, *Biochem. Biophys. Res. Commun.* **2002**, *291*, 813.
2 P. A. Zunszain, J. Ghuman, T. Komatsu, E. Tsuchida, S. Curry, *BMC Struct. Biol.* **2003**, *3*, 6.
3 E. Monzani, B. Bonafe, A. Fallarrini, C. Redaelli, L. Casella, L. Minchiotti, M. Galliano, *Biochim. Biophys. Acta* **2001**, *1547*, 302.
4 a) T. Komatsu, N. Ohmichi, P. A. Zunszain, S. Curry, E. Tsuchida, *J. Am. Chem. Soc.* **2004**, *126*, 14304. b) T. Komatsu, N. Ohmichi, A. Nakagawa, P. A. Zunszain, S. Curry, E. Tsuchida, *J. Am. Chem. Soc.* **2005**, *127*, 15933. c) T. Komatsu, A. Nakagawa, P. A. Zunszain, S. Curry, E. Tsuchida, *J. Am. Chem. Soc.* **2007**, *129*, 11286. d) Nakagawa, T. Komatsu, S. Curry, E. Tsuchida, *Org. Biomol. Chem.* **2009**, *7*, in press.
5 The picture was produced using PyMOL, W. L. DeLano, *The PyMOL Molecular Graphics System*, DeLano Scientific, San Carlos, CA, **2002**.
6 Supporting Information is available electronically on the CSJ-Journal Web site, http://www.csj.jp/journals/chem-lett/index.html.
7 E. Antonini, M. Brunori, *Hemoglobin and Myoglobin in Their Reactions with Ligands*, North-Holland Pub. Com., Amsterdam, **1971**, p. 18.
8 T. G. Traylor, C. K. Chang, J. Geibel, A. Berziniz, T. Mincey, J. Cannon, *J. Am. Chem. Soc.* **1979**, *101*, 6716.
9 Q. H. Gibson, *J. Biol. Chem.* **1970**, *245*, 3285.
10 J. S. Olson, M. E. Andersen, Q. H. Gibson, *J. Biol. Chem.* **1971**, *246*, 5919.
11 R. Rohlfs, A. J. Mathews, T. E. Carver, J. S. Olson, B. A. Springer, K. D. Egeberg, S. G. Sligar, *J. Biol. Chem.* **1990**, *265*, 3168.
12 K. Imai, H. Morimoto, M. Kotani, H. Watari, W. Hirata, M. Kuroda, *Biochim. Biophys. Acta* **1970**, *200*, 189.

Published on the web (Advance View) June 27, 2009; doi:10.1246/cl.2009.776

The role of an amino acid triad at the entrance of the heme pocket in human serum albumin for O_2 and CO binding to iron protoporphyrin IX†

Teruyuki Komatsu,*[a,b] Akito Nakagawa,[a] Stephen Curry,[c] Eishun Tsuchida,[a] Kenichi Murata,[d] Nobuhumi Nakamura[d] and Hiroyuki Ohno[d]

Received 19th May 2009, Accepted 29th June 2009
First published as an Advance Article on the web 22nd July 2009
DOI: 10.1039/b909794e

Complexation of iron(II) protoporphyrin IX (Fe^{2+}PP) into a genetically engineered heme pocket on recombinant human serum albumin (rHSA) creates an artificial hemoprotein which can bind O_2 reversibly at room temperature. Here we highlight a crucial role of a basic amino acid triad the entrance of the heme pocket in rHSA (Arg-114, His-146, Lys-190) for O_2 and CO binding to the prosthetic Fe^{2+}PP group. Replacing His-146 and/or Lys-190 with Arg resolved the structured heterogeneity of the possible two complexing modes of the porphyrin and afforded a single O_2 and CO binding affinity. Resonance Raman spectra show only one geometry of the axial His coordination to the central ferrous ion of the Fe^{2+}PP.

Introduction

Hemin [iron(III) protoporphyrin IX (Fe^{3+}PP), Fig. 1] dissociated from methemoglobin (metHb) is potentially toxic in the human body, because it intercalates in phospholipid membranes and participates in Fenton's reaction to produce hydroxyl radicals.[1] Hemopexin (Hpx, 60,000 Da), a β-glycoprotein in plasma (< 17 μM), captures the Fe^{3+}PP with an extraordinarily high binding affinity ($K > 10^{12}$ M^{-1}) and transports it to the liver for catabolism.[2] When Hpx becomes saturated (*e.g.* as a result of serious hemolytic injuries), the Fe^{3+}PP is first bound by human serum albumin (HSA, 66,500 Da) ($K = 1.1 \times 10^8$ M^{-1}),[3,4] the most abundant plasma protein (*ca.* 650 μM), and then transferred to Hpx. The biological function of the HSA–Fe^{3+}PP complex has attracted considerable interest for many years. However, Casella *et al.* reported little peroxidase or catalase activity,[5] so this naturally occurring hemoprotein may not play any significant role in vivo. If anything, HSA may serve to keep the incorporated hemin group physiologically silent.

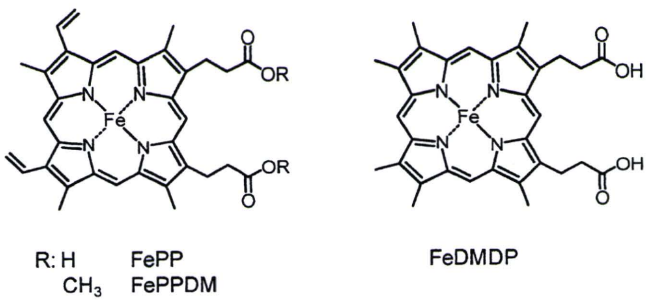

Fig. 1 Chemical formula of Fe porphyrins.

Crystal structure analysis of HSA–Fe^{3+}PP revealed that Fe^{3+}PP is bound within a deep hydrophobic slot in subdomain IB of HSA with axial coordination to the side-chain hydroxyl of Tyr-161 and salt bridges between the porphyrin propionates and a triad of basic amino acid residues at the pocket entrance (Arg-114, His-146, and Lys-190) (Fig. 2).[6,7] While the reduced ferrous HSA–Fe^{2+}PP is immediately autoxidized by O_2,[5] we found that a pair of site-specific mutations into the subdomain IB of HSA allows the Fe^{2+}PP to bind O_2: introduction of a proximal His at the Leu-185 position and substitution of the coordinated Tyr-161 with non-polar Leu (Y161L/L185H [rHSA**1**]) (Fig. 2).[9b,d] Remarkably, introduction of the proximal His at the Ile-142 position (on the opposite side of the porphyrin ring plane) also confers O_2 binding capability to the Fe^{2+}PP (I142H/Y161L [rHSA**2**]).[9a,c,d] These albumin O_2 transporters may serve as an effective red blood cell (RBC) substitute if the O_2 binding affinity is sufficient for clinical use. However, rHSA**1**–Fe^{2+}PP and rHSA**2**–Fe^{2+}PP both show two O_2 binding affinities ($P_{1/2}{}^{O2}$). The major component (species I, 60–75%) exhibits similar $P_{1/2}{}^{O2}$ to that of human RBC ($P_{1/2}{}^{O2} = 8$ Torr), but the minor component (species II, 25–40%) shows only a seventh to a tenth of the affinity (Table 1).[9] Our explanation for this observation is that the porphyrin plane of Fe^{2+}PP binds in the pocket in either of two alternative orientations (180° rotational isomers) that have slightly different geometries of axial His coordination to the central ferrous ion, only one of which confers high affinity O_2 binding.[9] Since less than 20% of species II of rHSA**2**–Fe^{2+}PP ($P_{1/2}{}^{O2} = 134$ Torr) is dioxygenated in the human lung's conditions ($P_{O2} = ca.$ 110 Torr, 37 °C), the low O_2 binding affinity component cannot effectively deliver O_2 to the tissues and should be excluded to develop this promising O_2 carrying plasma protein as an RBC substitute. Interestingly, a similar dependence of O_2 binding affinities on the orientations of the porphyrin ring

[a]*Research Institute for Science and Engineering, Waseda University, 3-4-1 Okubo, Shinjuku-ku, Tokyo, 169-8555, Japan. E-mail: teruyuki@waseda.jp; Fax: (+81) 3 5286 3148*
[b]*PRESTO, Japan Science and Technology Agency (JST), Japan. 4-1-8 Honcho, Kawaguchi-shi, Saitama, 332-0012, Japan*
[c]*Biophysics Section, Blackett Laboratory, Imperial College London, Exhibition Road, London, SW7 2AZ, United Kingdom*
[d]*Department of Biotechnology and Life Science, Tokyo University of Agriculture and Technology, 2-24-16, Naka-cho, Koganei-shi, Tokyo 184-8588, Japan*

† Electronic supplementary information (ESI) available: UV-vis absorption spectral data of rHSA–FePP and rHSA–FeDMDP, and absorption decay of CO rebinding to rHSA**2**–Fe^{2+}DMDP after laser flash photolysis. See DOI: 10.1039/b909794e

Table 1 O_2 and CO binding parameters of rHSA–Fe^{2+}PP in 50 mM potassium phosphate buffered solution (pH 7.0) at 22 °C

	k_{on}^{O2} ($\mu M^{-1}s^{-1}$)	k_{off}^{O2} (ms^{-1})		$P_{1/2}^{O2}$ (Torr)		k_{on}^{CO} ($\mu M^{-1}s^{-1}$)		k_{off}^{CO} (s^{-1})		$P_{1/2}^{CO}$ (Torr)	
		I	II	I	II	I	II	I	II	I	II
rHSA1–Fe^{2+}PP[a]	31	0.20	2.1	4	41	3.7	0.35	0.012	0.077	0.0026	0.18
rHSA2–Fe^{2+}PP[a]	7.5	0.22	1.7	18	134	2.0	0.27	0.013	0.079	0.0053	0.24
rHSA1(H146R)–Fe^{2+}PP	43	0.37	—	6	—	5.1	—	0.013	—	0.0033	—
rHSA1(L190R)–Fe^{2+}PP	24	0.35	—	9	—	4.0	—	0.010	—	0.0031	—
rHSA1(H146R/K190R)–Fe^{2+}PP	42	0.41	—	6	—	6.1	—	0.011	—	0.0022	—
rHSA2(H146R/K190R)–Fe^{2+}PP	11	0.30	—	17	—	1.7	—	0.012	—	0.0058	
Mb[b]	14	0.012		0.51		0.51		0.019		0.030	

[a] Ref. 9b. [b] Sperm whale Mb in 0.1 M potassium phosphate buffer (pH 7.0, 20 °C); ref. 17.

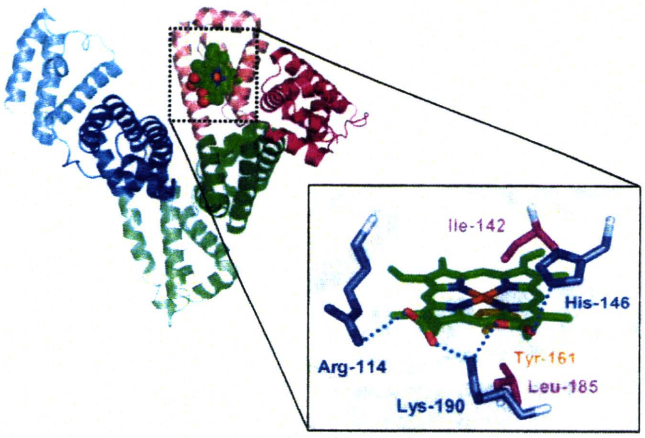

rHSA	Position				
	142	146	161	185	190
Wild type (WT)	Ile	His	Tyr	Leu	Lys
1	Ile	His	Leu	His	Lys
2	His	His	Leu	Leu	Lys
1(H146R)	Ile	Arg	Leu	His	Lys
1(K190R)	Ile	His	Leu	His	Arg
1(H146R/K190R)	Ile	Arg	Leu	His	Arg
2(H146R/K190R)	His	Arg	Leu	Leu	Arg

Fig. 2 Structure of the heme pocket in the rHSA(WT)–hemin complex (PDB ID: 1O9X from ref. 7).[8] Positions of the amino acids where site-specific mutations were introduced and abbreviations of the mutants are shown in the table.

plane is found in insect Hb.[10] If one could prepare a desired heme pocket architecture to distinguish the two possible binding modes of the asymmetric Fe^{2+}PP, it would provide new insights into the modulation of hemoprotein chemistry.

In this paper we report for the first time a role for the basic amino acid triad at the entrance of the heme pocket in rHSA in regulating O_2 and CO binding to the prosthetic Fe^{2+}PP group. Replacing His-146 and/or Lys-190 with Arg in rHSA**1**–Fe^{2+}PP and rHSA**2**–Fe^{2+}PP resolved the structural heterogeneity of the porphyrin plane orientation and afforded a single high-affinity O_2 and CO binding equilibrium. Moreover, the O_2 binding affinities of these hemoproteins are all similar to that of RBC. Resonance Raman (RR) spectra clearly show one geometry of the axial His coordination to Fe^{2+}PP.

Results and discussion

Design of the heme pocket

To bind the hemin molecule tightly, HSA exploits multiple electrostatic interactions between three basic amino acid residues and the hemin propionates at the wide entrance of the heme pocket (Fig. 2). Lys-190 adopts a central position and makes salt bridges to both propionic acid side chains. His-146 and Arg-114 provide a second electrostatic coordination with each carboxylate. Notably, the UV-vis absorption spectrum of HSA complexed with an iron(III) protoporphyrin IX dimethylester (Fe^{3+}PPDM, Fig. 1) showed very broad Soret and Q bands, suggesting that Fe^{3+}PPDM without peripheral carboxylic acids may not be bound stably within subdomain IB. This suggested that modification of this key basic amino acid triad involved in coordinating the hemin propionates could be used to regulate the orientation of the porphyrin ring plane in subdomain IB. We designed four new rHSA mutants based on the existing pair of double mutants that contain the substitutions necessary to confer O_2 binding to the Fe^{2+}PP (Y161L/L185H or I142H/Y161L).[9] His-146 and Lys-190 were replaced by more bulky and basic Arg: H146R, K190R, and H146R/K190R mutations were combined with the O_2 binding mutations (see Fig. 2 for details). We postulated that the introduction of Arg residues would reduce the space available at the entrance to the cavity and might thereby restrict the binding of Fe^{2+}PP to a single conformation.

Site-specific mutations were introduced into the HSA coding region in a plasmid vector (pHIL-D2 HSA). The proteins were expressed in the yeast species *Pichia pastoris*. The rHSA–Fe^{2+}PP complexes were prepared according to our previously reported procedures (see Experimental).

O_2 and CO binding properties of rHSA–Fe^{2+}PP

The UV-vis absorption spectra of all six rHSA(mutant)–Fe^{3+}PP were essentially identical (Fig. 3, Table S1†). They were easily reduced to the corresponding ferrous complexes by adding a small amount of degassed aqueous $Na_2S_2O_4$ under an N_2 atmosphere. A single broad absorption band (λ = 558–559 nm) in the visible region signified the formation of a five-*N*-coordinate high-spin complex similar to deoxy Mb[11] or the synthetic chelated heme in DMF.[12] The spectral features and amplitude did not change in the temperature range of 5–25 °C. These observations show that the guanidinium groups of Arg-146 or Arg-190 do *not* interact with

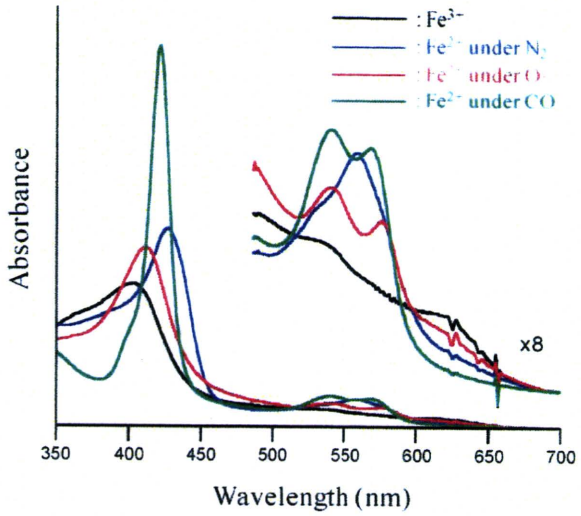

Fig. 3 UV-vis absorption spectral changes of rHSA1(H146R/K190R)–Fe^{2+}PP in 50 mM potassium phosphate buffered solution (pH 7.0) at 22 °C.

the ferrous iron of the Fe^{2+}PP, since the resulting formation of a six-*N*-coordinate low-spin complex would have yielded sharp and split α, β bands in the visible region[9c] and been sensitive to rapid oxidation by O_2 *via* an outer sphere mechanism.[13]

Upon exposure of the rHSA–Fe^{2+}PP solution to O_2 gas, the UV-vis absorption changed to that of the dioxygenated complex (Fig. 3).[9,11] After exposure to flowing CO, the Fe^{2+}PP produced a typical carbonyl complex.

We then used laser flash photolysis spectroscopy to determine association and dissociation rate constants (k_{on}, k_{off}) for O_2 and CO binding to rHSA–Fe^{2+}PP.[9] The time dependence of the absorption change accompanying the CO recombination to rHSA**1**–Fe^{2+}PP and rHSA**2**–Fe^{2+}PP obeyed double-exponentials, although the O_2 binding kinetics followed a single-exponential.[9] The slow phase (species II) of the CO rebinding showed 7–11-fold lower k_{on}^{CO} and 6-fold higher k_{off}^{CO} than those of the fast phase (species I) (Table 1). We interpreted this to mean that the low O_2 binding affinity conformers of rHSA**1**–Fe^{2+}PP and rHSA**2**–Fe^{2+}PP have bending strain in the proximal His coordination.[9,14–16] In contrast, the rebinding kinetics of O_2 and CO to rHSA**1**(H146R)–Fe^{2+}PP, rHSA**1**(K190R)–Fe^{2+}PP, rHSA**1**(H146R/K190R)–Fe^{2+}PP and rHSA**2**(H146R/K190R)–Fe^{2+}PP were strictly monophasic (Fig. 4). As a result, these hemoproteins showed single O_2 and CO binding affinity ($P_{1/2}^{O2}$ and $P_{1/2}^{CO}$), which were all similar to the higher affinities (species I) of the original double mutants (Table 1). We can conclude that the introduction of Arg into the entrance of the heme pocket of rHSA**1** and rHSA**2** is effective at excluding the low O_2 binding affinity conformer.

CO binding to rHSA–Fe^{2+}DMDP

To verify our interpretation that the replacement of H146 and/or K190 by Arg resolved the structural heterogeneity of the two complexing modes of the Fe^{2+}PP and gave a single O_2 and CO binding affinity, we examined the incorporation of a symmetrical iron(II) 2,4-dimethyl-deuteroporphyrin (Fe^{2+}DMDP, Fig. 1) as an active site. The UV-vis absorption spectrum of

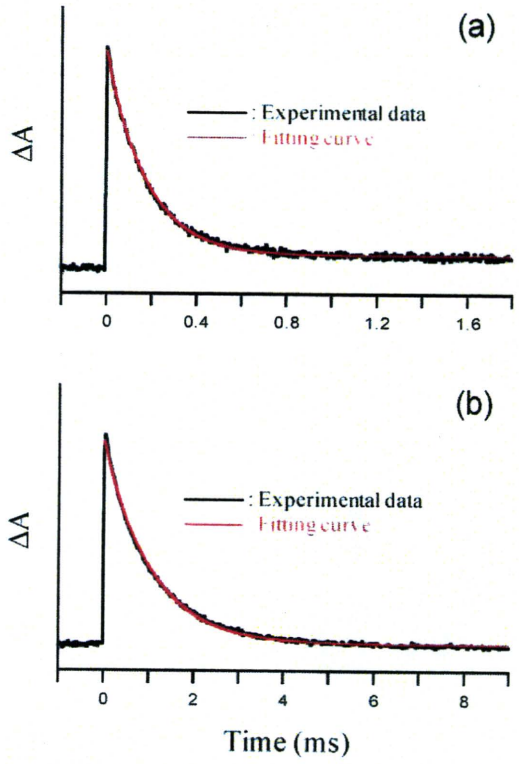

Fig. 4 Absorption decay of O_2 and CO rebinding to rHSA1(H146R/K190R)–Fe^{2+}PP after the laser flash photolysis at 22 °C; (a) O_2 and (b) CO. Both kinetics were composed of monophasic phases. A relaxation curve was fitted single exponential (red line).

the ferric rHSA**2**–Fe^{3+}DMDP showed a very similar pattern to that of rHSA**2**–Fe^{3+}PP though each λ_{max} value was hypsochromic (8–11 nm) shifted (Table S1†). The reduced ferrous form of rHSA**2**–Fe^{2+}DMDP under an N_2 atmosphere exhibited a slightly broadened Soret band absorption, but the main species was a five-*N*-coordinate high spin complex involving axial His-142 coordination. Upon introduction of O_2 gas through the solution, rHSA**2**–Fe^{2+}DMDP bound O_2 only at 5 °C and was observed to autoxidize at 22 °C. In general, the stability of the O_2 adduct complex of a heme derivative is sensitive to the electron density at Fe^{2+} and thus to the substituents at the porphyrin periphery.[18,19] Our attempt to determine the O_2 binding parameters of rHSA**2**–Fe^{2+}DMDP unfortunately failed. However, after introduction of CO gas, rHSA**2**–Fe^{2+}DMDP produced a stable carbonyl complex. We again used laser flash photolysis to characterize the CO binding properties of this hemoprotein. As expected, the absorption decay associated with CO recombination with rHSA**2**–Fe^{2+}DMDP was clearly monophasic (Fig. S1†). This result implied that the symmetric Fe^{2+}DMDP molecule is accommodated in subdomain IB of rHSA**2** in a single orientation and there is only one geometry of the axial His-142 coordination to the central ferrous ion of Fe^{2+}DMDP. Interestingly, the CO rebinding to rHSA**2**–Fe^{2+}DMDP (k_{on}^{CO}: 0.42 $\mu M^{-1}s^{-1}$) was relatively slow compared to that of rHSA**2**–Fe^{2+}PP and similar to Mb.[17]

RR and IR spectroscopies

The RR and infrared (IR) spectra of these artificial hemoproteins also supported the results described above. The stretching

frequencies of the carbonyl complex [ν(Fe–CO) and ν(CO)] provide crucial information about the Fe–trans ligand bond.[20,21] The high-frequency region of the RR spectra of rHSA1–Fe^{2+}PP(CO) and rHSA1(H146R/K190R)–Fe^{2+}PP(CO) both exhibited an intense peak at 1373 cm^{-1} (λ_{ex}: 413.1 nm), which indicates a deformed pyrrole-ring breathing-like mode (ν_4) and corresponds well to the value of the 6-coordinate low-spin carbonyl complex.[21a] However, while the low-frequency RR spectra of rHSA1–Fe^{2+}PP(CO) exhibited two ν(Fe–CO) bands at 493 and 525 cm^{-1}, rHSA1(H146R/K190R)–Fe^{2+}PP (CO) showed only a single ν(Fe–CO) band at 493 cm^{-1} (Fig. 5).[22] Since it is known that the weaker the Fe-trans ligand coordination, the stronger the Fe–CO bond in the carbonyl complex,[20] we assigned the higher 525 cm^{-1} band of rHSA1–Fe^{2+}PP(CO) to the low CO binding affinity conformer. The 493 cm^{-1} band was therefore assigned to the high affinity conformer, in which the proximal His-185 coordinates to the Fe^{2+}PP without unfavourable strain.

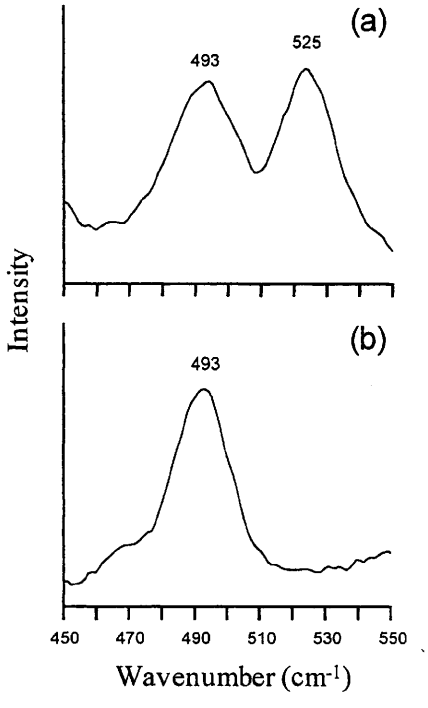

Fig. 5 Resonance Raman spectra of (a) rHSA1–Fe^{2+}PP(CO) and (b) rHSA1(H146R/K190R)–Fe^{2+}PP(CO) in 50 mM potassium phosphate buffered solution (pH 7.0) at 22 °C.

Regarding IR spectra, the ν(CO) vibration appeared at 1963 cm^{-1} for rHSA1–Fe^{2+}PP(CO) and at 1967 cm^{-1} for rHSA1(H146R/K190R)–Fe^{2+}PP(CO). Spiro *et al.* prepared a systematic plot of ν(Fe–CO) *versus* ν(CO) for a large number of carbonyl heme complexes and found a single inverse correlation when imidazole is the axial ligand.[21b,c] This is attributed to back donation of Fe^{2+} dπ electrons to the CO π* orbital. The relationship between ν(Fe–CO) and ν(CO) for rHSA1(H146R/K190R)–Fe^{2+}PP(CO) fits on the line for the imidazole complexes.[21b,c] On the other hand, the low O_2 binding component of rHSA1–Fe^{2+}PP(CO) showed a positive deviation from the line. This result again indicates a very weak electron donation from the proximal His-185 in the low O_2 binding conformer.

Conclusions

We prepared rHSA–Fe^{2+}PP complexes having a single O_2 and CO binding affinity by introducing Arg into the His-146 and/or Lys-190 positions. These artificial hemoproteins have a uniform Fe^{2+}PP orientation and His ligation (His-185 or His-142) geometry to the central ferrous ion without inclination. The key triad of the basic amino acid residues (Arg-114, His-146 and Lys-190) at the entrance of the heme pocket of HSA plays an important role in stabilizing the porphyrin molecule *via* salt-bridge formation and might also discriminate the two sides of the porphyrin ring. In mammals, His-146 is universally conserved, but Lys-190 is present only in primate albumin. The wild-type HSA statistically accommodates the hemin in alternative orientations; the discrimination of the porphyrin plane by serum albumin might be unnecessary for the evolution process. But the engineering of an rHSA–Fe^{2+}PP complex with a single O_2 binding affinity is potentially of tremendous clinical importance for blood substitutes and O_2-transporting therapeutic reagents.

Experimental

Materials and apparatus

All materials were used as purchased without further purification. Iron(III) protoporphyrin IX chloride (Fe^{3+}PP) was purchased from Fluka. Iron(III) protoporphyrin IX dimethyl ester chloride (Fe^{3+}PPDM) was synthesized from protoporphyrin IX dimethyl ester (Sigma). Iron(III) 2,4-dimethyl-deuteroporphyrin chloride (Fe^{3+}DMDP) was synthesized from 2,4-dimethyl-deuteroporphyrin dimethyl ester (Frontier Scientific).[23] UV-vis absorption spectra were obtained on an Agilent 8453 UV-visible spectrophotometer equipped with an Agilent 89090A temperature control unit. Kinetic measurements for the O_2 and CO bindings were carried out on a Unisoku TSP-1000WK time-resolved spectrophotometer with a Spectron Laser Systems SL803G-10 Q-switched Nd:YAG laser, which generated a second-harmonic (532 nm) pulse of 6-ns duration (10 Hz). A 150 W xenon arc lamp was used as the probe light source. The gas mixture with the desired partial pressure of O_2/CO/N_2 was prepared by a Kofloc Gasblender GB-3C. Resonance Raman spectra of the carbonyl rHSA–Fe^{2+}PP complexes were obtained on a JASCO NRS-1000 spectrophotometer using a Kaiser Optical Holographic Notch-Plus filter and a liquid N_2-cooled CCD detector. The excitation source was a Coherent Innova 90C Kr^+ laser. Infrared spectra of the carbonyl rHSA–Fe^{2+}PP complex were obtained on a JASCO FT/IR-4200 spectrophotometer.

Preparation of rHSA

The designed rHSAs were prepared according to our previously reported techniques.[9b] The mutations (H146R and/or K190R) were introduced into the rHSA coding region in a plasmid vector encoding the double mutant [rHSA1 or rHSA2] by use of the Stratagene QuikChange mutagenesis kit. All mutations were confirmed by DNA sequencing. The plasmid was then digested by NotI and introduced into yeast (*Pichia pastoris* GS115) by electroporation. The expression protocols and media formulations were as previously described.[9b] The expressed proteins were harvested from the growth medium by precipitation with ammonium sulfate

and purified by a Cibacron Blue column of Blue Sepharose 6 Fast Flow (Amersham Pharmacia Biotech). After concentration using a Vivaspin 20 ultrafilter (10 kDa M_w cutoff), the samples were applied to a Superdex 75 column (Amersham Pharmacia Biotech) using 50 mM potassium phosphate as the running buffer. The purification steps were followed by SDS-PAGE analysis. The purified rHSA was lyophilized and stored in the freezer at −20 °C.

Preparation of rHSA–Fe^{2+}porphyrin

Typically 5 mL of 0.1 mM rHSA in 50 mM potassium phosphate (pH 7.0) was mixed with 0.8 mL of 0.688 mM Fe^{3+}PP in DMSO (Fe^{3+}PP : rHSA was molar ratio of 1:1) and incubated overnight with rotation in the dark at room temperature. The complex was then diluted with 50 mM potassium phosphate (*ca.* 15 mL) and concentrated to the initial volume (5.8 mL) using a Vivaspin 20 ultrafilter (10 kDa M_w cutoff). These dilution and concentration cycles were repeated to reduce the final concentration of DMSO to *ca.* <0.001 vol%. The rHSA–Fe^{2+}PPDM and rHSA–Fe^{2+}DMDP were also prepared in the same manner. The 50 mM phosphate buffered solution (pH 7.0) of rHSA–Fe^{3+}PP ([Fe^{3+}PP]: *ca.* 10 μM) in a 10 mm path length optical quartz cuvette sealed with a rubber septum was purged with N_2 for 30 min. A small excess amount of degassed aqueous sodium dithionite was added by microsyringe to the sample under an N_2 atmosphere to reduce the central ferric ion of the Fe^{3+}PP, generating the deoxy ferrous rHSA–Fe^{2+}PP.

Determination of O_2 and CO binding parameters

The O_2 and CO recombination with rHSA–Fe^{2+}PP after nanosecond laser flash photolysis of the dioxygenated or carbonyl complex occurs according to eqn (1) with the association rate constant (k_{on}^{L}) and dissociation rate constant (k_{off}^{L}) (where L: O_2 or CO).

$$Fe^{2+}PP\text{-}L \xrightarrow{h\nu} Fe^{2+}PP + L \underset{k_{off}^{L}}{\overset{k_{on}^{L}}{\rightleftharpoons}} Fe^{2+}PP\text{-}L \qquad (1)$$

$$[P_{1/2}^{L} = (K^{L})^{-1} = (k_{on}^{L}/k_{off}^{L})^{-1}]$$

The k_{on}^{CO} was measured by following the absorption at 436 nm for Fe^{2+}PP(CO) or 411 nm for Fe^{2+}DMDP(CO) after laser pulse irradiation to the carbonyl complex at 22 °C. The k_{on}^{O2} and O_2 binding equilibrium constant [$K^{O2} = (P_{1/2}^{O2})^{-1}$)] can be determined by a competitive rebinding technique by use of gas mixtures with different partial pressures of O_2/CO/N_2 at 22 °C. The relaxation curves that accompanied the O_2 or CO recombination were analyzed by single or double exponential profiles with Unisoku Spectroscopy & Kinetics software. The k_{off}^{O2} was calculated from k_{on}^{O2}/K^{O2}. The k_{off}^{CO} was measured by displacement with NO for the carbonyl complex at 22 °C. The time course of the UV-vis absorption change that accompanied the CO-dissociation was fitted to single or double exponential. The CO binding constants [$K^{CO} = (P_{1/2}^{CO})^{-1}$] were calculated from k_{off}^{CO}/k_{on}^{CO}.

Raman spectroscopy

Spectra of the carbonyl complexes of rHSA–Fe^{2+}PP ([Fe^{2+}PP]: 2–4 mM in 50 mM phosphate buffered solution (pH 7.0)) were collected using back-scattering geometry at an excitation wavelength of λ_{ex}: 413.1 nm. The laser power for the samples was 1.8 mW. Each spectrum was recorded with 20 s accumulation time at 22 °C, and ten repetitively measured spectra were averaged to improve the signal to noise ratio. Peak frequencies were calibrated relative to indene and CCl_4 as a standard and were accurate to 1 cm^{-1}.

IR spectroscopy

The IR spectra of the carbonyl complexes of rHSA–Fe^{2+}PP ([Fe^{2+}PP]: 2–4 mM in 50 mM phosphate buffered solution (pH 7.0)) were obtained in CaF_2 cells (JASCO, path length: 0.025 mm). The cell containing water was used for the reference. The spectrum was accumulated 64 times to improve its signal-to-noise ratio.

Acknowledgements

This work was partially supported by Grant-in-Aid for Scientific Research (No. 20750142, 20350058) from JSPS, PRESTO from JST, and Health Science Research Grants (Regulatory Science) from MHLW Japan.

Notes and references

1 V. Jeney, J. Balla, A. Yachie, G. M. Vercellotti, J. W. Eaton and G. Balla, *Blood*, 2002, **100**, 879.
2 E. Tolosano and F. Altruda, *DNA Cell Biol.*, 2002, **21**, 297.
3 T. Peters, *All about Albumin: Biochemistry, Genetics and Medical Applications*, Academic Press, San Diego, 1996, and references therein.
4 P. A. Adams and M. C. Berman, *Biochem. J.*, 1980, **191**, 95.
5 E. Monzani, B. Bonafe, A. Fallarrini, C. Redaelli, L. Casella, L. Minchiotti and M. Galliano, *Biochim. Biophys. Acta*, 2001, **1547**, 302.
6 M. Wardell, Z. Wang, J. X. Ho, J. Robert, F. Ruker, J. Ruble and D. C. Carter, *Biochem. Biophys. Res. Commun.*, 2002, **291**, 813.
7 P. A. Zunszain, J. Ghuman, T. Komatsu, E. Tsuchida and S. Curry, *BMC Struct. Biol.*, 2003, **3**, 6.
8 The picture was produced using PyMOL, W. L. DeLano, *The PyMOL Molecular Graphics System*, DeLano Scientific, San Carlos, CA, 2002.
9 (*a*) T. Komatsu, N. Ohmichi, P. A. Zunszain, S. Curry and E. Tsuchida, *J. Am. Chem. Soc.*, 2004, **126**, 14304; (*b*) T. Komatsu, N. Ohmichi, A. Nakagawa, P. A. Zunszain, S. Curry and E. Tsuchida, *J. Am. Chem. Soc.*, 2005, **127**, 15933; (*c*) T. Komatsu, A. Nakagawa, P. A. Zunszain, S. Curry and E. Tsuchida, *J. Am. Chem. Soc.*, 2007, **129**, 11286; (*d*) T. Komatsu, A. Nakagawa and E. Tsuchida, *Macromol. Symp.*, 2008, **270**, 187.
10 K. Gersonde, H. Sick, M. Overkamp, K. M. Smith and D. W. Parish, *Eur. J. Biochem.*, 1986, **157**, 393.
11 E. Antonini and M. Brunori, *Hemoglobin and Myoglobin in Their Reactions with Ligands*, North-Holland: Amsterdam, 1971, p 18.
12 T. G. Traylor, C. K. Chang, J. Geibel, A. Berzinis, T. Mincey and J. Cannon, *J. Am. Chem. Soc.*, 1979, **101**, 6716.
13 M. M. L. Chu, C. E. Castro and G. M. Hathaway, *Biochemistry*, 1978, **17**, 481.
14 From numerous investigations on synthetic model hemes, it has been shown that a bending strain in the proximal base coordination to the central Fe^{2+} atom, the "proximal-side steric effect", can increase the k_{off}^{CO} and decrease k_{on}^{CO}, whereas it increases k_{off}^{O2} without greatly altering the kinetics of O_2 association[14,15].
15 J. P. Collman, J. I. Brauman, B. L. Iverson, J. L. Sessler, R. M. Morris and Q. H. Gibson, *J. Am. Chem. Soc.*, 1983, **105**, 3052.
16 T. G. Traylor, S. Tsuchiya, D. Campbell, M. Mitchel, D. Stynes and N. Koga, *J. Am. Chem. Soc.*, 1985, **107**, 604.
17 R. Rohlfs, A. J. Mathews, T. E. Carver, J. S. Olson, B. A. Springer, K. D. Egeberg and S. G. Sligar, *J. Biol. Chem.*, 1990, **265**, 3168.
18 T. G. Traylor, D. K. White, D. H. Campbell and A. P. Berzinis, *J. Am. Chem. Soc.*, 1981, **103**, 4932.

19 A. Nakagawa, N. Ohmichi, T. Komatsu and E. Tsuchida, *Org. Biomol. Chem.*, 2004, **2**, 3108.
20 E. A. Kerr, H. C. Mackin and N.-T. Yu, *Biochemistry*, 1983, **22**, 4373.
21 (*a*) T. G. Spiro and J. M. Burke, *J. Am. Chem. Soc.*, 1976, **988**, 5482; (*b*) X.-Y. Li and T. G. Spiro, *J. Am. Chem. Soc.*, 1988, **110**, 6024; (*c*) K. M. Vogel, P. M. Kozlowski, M. Z. Zgierski and T. G. Spiro, *Inorg. Chim. Acta*, 2000, **297**, 11.
22 These peaks are not the stretching mode of a disulfide bond [ν(S–S)]. It is observed at 500–545 cm^{-1} in the Raman spectrum of protein (λ_{ex}: 532 nm). Although there are 17 S–S bridges in HSA, our spectra of rHSAs without heme exhibited no peak in that region. C. David, S. Foley, C. Mavon and M. Enescu, *Biopolymers*, 2008, **89**, 623.
23 K. M. Smith and L. A. Kehres, *J. Chem. Soc., Perkin Trans. 1*, 1983, 2329.

Drug Metab. Pharmacokinet. 24 (4): 287-299 (2009).

Review

Structural and Mutagenic Approach to Create Human Serum Albumin-Based Oxygen Carrier and Photosensitizer

Teruyuki KOMATSU[1,2,*], Akito NAKAGAWA[1] and Xue QU[1]

[1]*Research Institute for Science and Engineering, Waseda University, Tokyo, Japan*
[2]*PRESTO, Japan Science Technology Agency, Saitama, Japan*

Full text of this paper is available at http://www.jstage.jst.go.jp/browse/dmpk

Summary: Human serum albumin (HSA) is a versatile protein found at high concentration in blood plasma and binds a range of insoluble endogenous and exogenous compounds. We have shown that complexation of functional molecules into HSA creates unique proteins never seen in nature. Complexing an iron-protoporphyrin IX into a genetically engineered heme pocket of recombinant HSA (rHSA) generates an artificial hemoprotein, which binds O_2 reversibly in much the same way as hemoglobin. A pair of site-specific mutations, (i) introduction of a proximal histidine at the Ile-142 position and (ii) substitution of Tyr-161 with Phe or Leu, allows the heme to bind O_2. Additional modification on the distal side of the heme pocket provides rHSA(triple mutant)-heme complexes with a variety of O_2 binding affinity. Complexing a carboxy-C_{60}-fullerene (CF) into HSA generates a protein photosensitizer for photodynamic cancer therapy. Energy transfer occurs from a photoexcited triplet-state of HSA-CF (HSA-^{3}CF*) to O_2, forming singlet oxygen ($^1O_2$). This protein does not show dark cytotoxicity, but induceds cell death under visible light irradiation.

Keywords: human serum albumin; oxygen carrier; photosensitizer; heme; site-directed mutagenesis; fullerene; singlet oxygen; photodynamic therapy

Introduction

Human serum albumin (HSA, Mw: 66.5 kDa) is the most prominent plasma protein in our bloodstream and is characterized by remarkable ability to bind a great variety of hydrophobic molecules.[1-3] Typical endogenous ligands for HSA are fatty acids, bilirubin, bile acids and thyroxine.[4-8] The protein binds a wide range of drugs. Hemin (Fe^{3+} protoporphyrin IX, **Fig. 1**) released from methemoglobin (metHb) during the enucleation of red blood cells (RBCs) is also captured by HSA. Free hemin is potentially toxic because it may catalyze hydroxyl radical formation. In 1938, Fairely verified that serum protein observed to bind the hemin was albumin and proposed the name "methemalbumin".[9] Muller-Eberhard and Morgan reported the UV-vis absorption spectrum of the HSA-hemin complex in 1975 and supposed formation of high-spin hemoprotein with an axial coordination of amino acid residue of the protein.[10] The binding constant for hemin to HSA was determined to be $1.1 \times 10^8\ M^{-1}$.[11] This strong affinity of HSA for hemin has stimulated efforts to develop HSA as an artificial hemoprotein which mimics the diverse biological reactivities of natural hemoproteins, such as O_2 transport of Hb. If the HSA-based O_2 carrier is realized, it has the potential of acting not only as an RBC substitute, but also an O_2-providing therapeutic reagent. However, it has taken over 60 years to confer the O_2 binding capability on the HSA-hemin complex since Fairely's finding.

HSA is composed of three structurally similar domains (I–III), each containing A and B subdomains.[12,13] Crystallographic studies reveal that hemin is bound within a narrow cavity in subdomain IB with an axial coordination of tyrosine to the central Fe^{3+} ion and electrostatic interactions between the porphyrin propionates and a triad of basic amino acid residues (**Fig. 2**).[14,15] In terms of the general hydrophobicity of this α-helical pocket, the subdomain IB of HSA has similar features to the heme binding site of Hb or myoglobin (Mb), namely "heme pocket". However, the reduced form of HSA-hemin is rapidly oxidized by O_2.[16]

It is of current interest to prepare albumin-based fake enzymes by exploiting the ligand binding properties of HSA.[16-19] Casella *et al.*, demonstrated the HSA-hemin

Received; April 9, 2009, Accepted; June 18, 2009
**To whom correspondence should be addressed:* Teruyuki KOMATSU, Ph.D., *Research Institute for Science and Engineering, Waseda University, 3-4-1 Okubo, Shinjuku-ku, Tokyo 169-8555, Japan. Tel & Fax. +81-3-5286-3148, E-mail: teruyuki@waseda.jp*

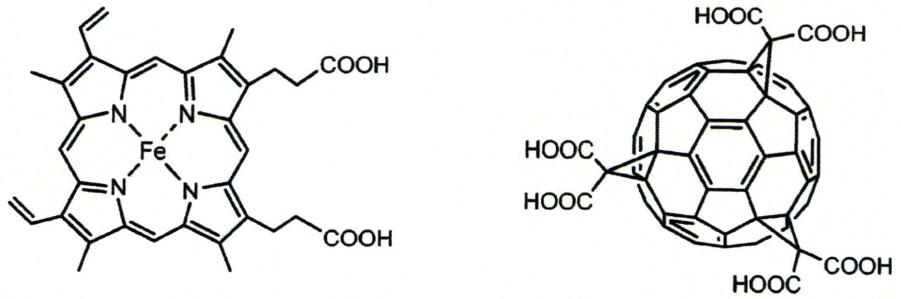

Fe^{2+}protoporphyrin IX (heme) Carboxy-C_{60}-fullerene (CF)

Fig. 1. Chemical formula of heme and CF

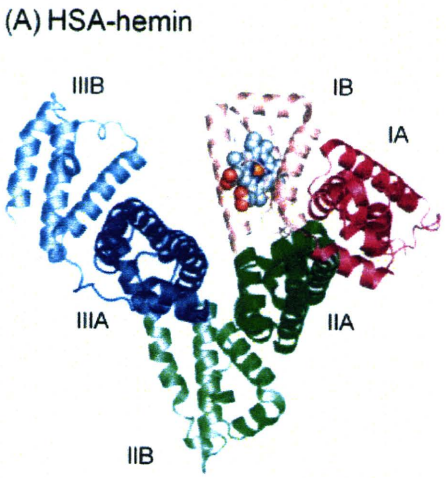

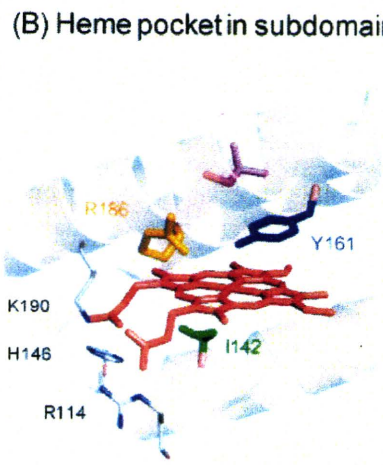

	Positions 142	161		
Wild type	I	Y	L	R
I142H/Y161F	H	F	L	R
I142H/Y161L	H	L	L	R
I142H/Y161F/L185N	H	F	N	R
I142H/Y161L/L185N	H	L	N	R
I142H/Y161F/L185Q	H	F	Q	R
I142H/Y161L/L185Q	H	L	Q	R
I142H/Y161F/L185H	H	F	H	R
I142H/Y161L/R186L	H	L	L	L
I142H/Y161L/R186F	H	L	L	F

Fig. 2. (A) Crystal structure of HSA-hemin complex (1O9X) from ref. 15. (B) Heme pocket structure in subdomain IB and positions of amino acids where site-specific mutations are introduced.
Abbreviations of triple mutants are shown in the table.

complex exhibited weak peroxidase and catalase activity.[16] Gross *et al.* showed that HSA incorporating Fe^{3+} corrole or Mn^{3+} corrole is useful for enantioselective sulfoxidation of prochiral sulfides by hydrogen peroxide (up to 74% ee).[17] Reets *et al.* used HSA-Cu^{2+} phthalocyanine as Lewis acidic catalyst for highly enantioselective Diels-Alder reactions of azachalcones (85–98% ee).[18] Moreover, Gozin *et al.* prepared bovine serum albumin-C_{60} fullerene hybrid using cyclodextrin-C_{60} intermediate.[19] We investigated HSA incorporating synthetic Fe^{2+} porphyrin (FeP) "HSA-FeP" as an entirely synthetic O_2 transporter.[20–39] A saline solution of HSA-FeP is a most promising material for RBC substitute. In this review, we describe very recent results on the O_2 carrier formed by complexing natural Fe^{2+} protoporphyrin IX (heme) with genetically engineered HSA and on photosensitizer formed by complexing carboxy-C_{60}-fullerene (CF) with HSA (**Fig. 1**).[40–43]

Recombinant HSA Mutants Complexed with Heme (rHSA-Heme) as Oxygen Carrier

Naturally occurring HSA-hemin complex: Crystal structure analysis revealed that hemin is bound within a narrow D-shaped hydrophobic cavity in subdomain IB of HSA where the central ferric ion is axially coordinated by Tyr-161 and the two propionate side-chains at the porphyrin periphery form salt-bridges with a triad of basic amino acid residues (Arg-114, His-146, Lys-190) (**Fig. 2**).[14,15] The UV-vis absorption spectrum of the HSA-hemin solution showed a Soret band at 405 nm and the $p\pi$-$d\pi$ charge-transfer (CT) band at 624 nm (**Fig. 3**). The dominant features of the spectrum were almost the same as those of previously reported HSA-hemin[10,16] and H93Y recombinant Mb [rMb(H93Y)], in which the proximal His-93 was changed to tyrosine.[44,45] Our absorption spectral data imply that the hemin is bound to Tyr-161 of HSA to form a ferric five-coordinate high-spin complex. Neverthless, CT absorptions of the HSA-hemin appeared at a higher wavelength (λ_{max}: 624 nm) compared to

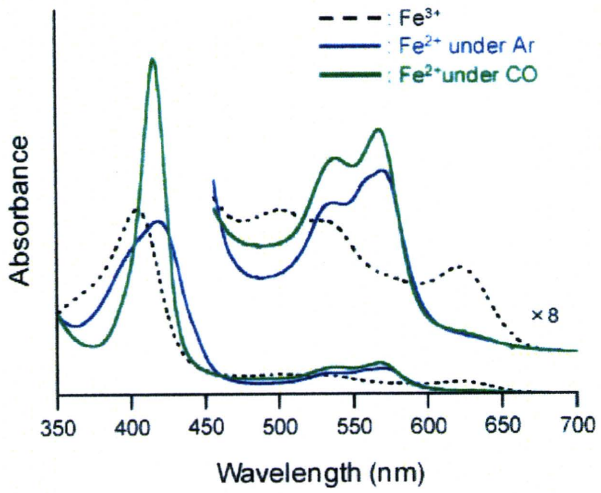

Fig. 3. UV-vis absorption spectral changes of the HSA-heme in 50 mM potassium phosphate buffered solution (pH 7.0)

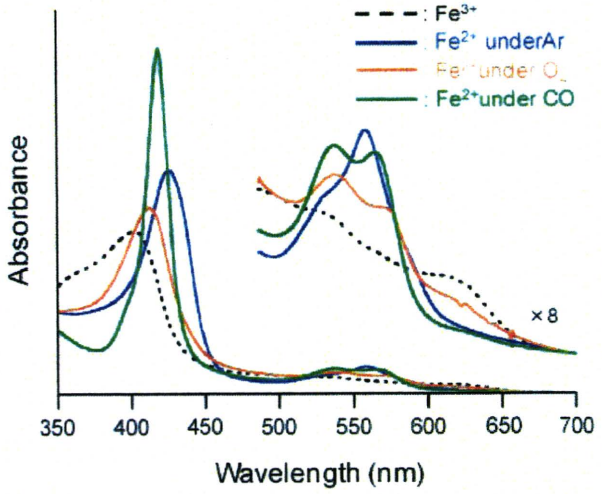

Fig. 4. UV-vis absorption spectral changes of the rHSA(I142H/Y161L)-heme in 50 mM potassium phosphate buffered solution (pH 7.0)

rMb(H93Y) (λ_{max}: 598–599 nm), which suggests that the axial coordination of Tyr-161 to the hemin is weaker than that of rMb(H93Y). The magnetic circular dichroism (MCD) spectra also support the formation of a five-coordinate high-spin hemin complex with weak Tyr-161 ligation in HSA-hemin.[41]

Reduction of the ferric HSA-hemin by the addition of aqueous sodium dithionite under an Ar atmosphere gave a ferrous heme complex with a Soret band at 419 nm and two definite Q bands at 538 and 570 nm (**Fig. 3**). Based on careful inspection of UV-vis and MCD spectra, we concluded that the ferrous HSA-heme is an unusual mixture of a five-coordinate high-spin complex with Tyr-161 and a four-coordinate intermediate-spin state under an Ar atmosphere. Smulevich *et al.* recently measured resonance Raman spectroscopy of the HSA-hemin complex and strongly supported our interpretation.[46]

Upon the addition of O_2 gas through this solution, the central ferrous ion was rapidly oxidized even at 5°C. This is due to the fact that HSA lacks the proximal histidine which enables the prosthetic heme group to bind O_2 in Hb and Mb.

rHSA(double mutant)-heme complexes: On the basis of the crystal structure of the HSA-hemin complex, we used site-directed mutagenesis to introduce a histidine into the heme binding site of HSA. This should provide axial coordination to the central Fe^{2+} atom of the heme and thereby promote O_2 binding. Tyr-161 was the first candidate for site-directed mutagenesis (**Fig. 2**), but our simulation results showed that the distance from N_ε(Y161H) to Fe(heme) would be too far (~4.0 Å). As an alternative, favorable positions for axial imidazole insertion would be Ile-142. The N_ε(I142H)-Fe distance was estimated to be 2.31 Å. We therefore designed and prepared rHSA mutants, rHSA(I142H/Y161F) and rHSA(I142H/Y161L) (**Fig. 2**) and evaluated the O_2 binding properties of the heme complexes.

The rHSA(double mutant)-hemin was easily reduced to the ferrous complex under an Ar atmosphere. A single broad Q band (λ_{max}: 559 nm) in the visible absorption of rHSA(I142H/Y161F)-heme and rHSA(I142H/Y161L)-heme was similar to that of deoxy Mb[47] or the synthetic chelated-heme in N,N-dimethylformamide (**Fig. 4**),[48] indicating the formation of a five-*N*-coordinate high-spin complex. The heme was incorporated into the artificial heme pocket with axial His-142 coordination. Upon exposure of the rHSA(I142H/Y161F)-heme and rHSA(I142H/Y161L)-heme solutions to O_2, the UV-vis absorptions changed to that of the O_2 adduct complex at 22°C (**Fig. 4**).[47,48] After flowing CO gas, these hemoproteins produced very stable carbonyl complexes. The single mutant rHSA(I142H)-heme which retains Y161, could not bind O_2. The polar phenolate residue at the top of the porphyrin plane probably accelerates the proton-driven oxidation of the Fe^{2+} center.

To evaluate the kinetics of O_2 and CO binding to rHSA(double mutant)-heme, laser flash photolysis experiments were carried out.[41,42,49,50] It is noteworthy that the absorbance decay accompanying CO recombination to rHSA(I142H/Y161F)-heme and rHSA(I142H/Y161L)-heme was composed of double-exponential profiles normally not seen in Mb. The rebinding of O_2 to the hemoproteins followed simple monophasic decay. Based on numbers from investigation on synthetic Fe^{2+} porphyrin models, it has been shown that a bending strain in the proximal histidine coordination to the central Fe^{2+} atom, "proximal-side steric effect", increases the dissociation rate and decreases the association rate for CO, whereas it increases the O_2 dissociation rate without changing the kinetics of O_2 association.[49,50] Our interpretation was that there may be two different geometries for axial

His-142 coordination to the central Fe^{2+} of the heme (species I and II), each one accounting for a component of biphasic kinetics of CO rebinding. The heme molecule appears to bind to subdomain IB in two orientation (180o rotational isomers), giving two different geometries for axial His-142 coordination.

The association and dissociation rate constants for O_2 or CO ($k_{on}^{O_2}$, $k_{off}^{O_2}$, k_{on}^{CO}, k_{off}^{CO}) and binding affinities for O_2 or CO [$P_{1/2}^{O_2}=(K^{O_2})^{-1}$, $P_{1/2}^{CO}=(K^{CO})^{-1}$] for the rHSA(mutant)-heme complexes (eq. 1) are summarized in **Table 1 and 2.**

$$\text{rHSA-heme} + L \underset{k_{off}^{L}}{\overset{k_{on}^{L}}{\rightleftarrows}} \text{rHSA-heme-L} \qquad (1)$$

$$(L = O_2 \text{ or CO})$$

$P_{1/2}^{O_2}$ of rHSA(I142H/Y161F)-heme and rHSA(I142H/Y161L)-heme were determined to be 3–18 and 31–134 Torr for species I (the first phase) and species II (the second phase), respectively. Even the O_2 binding affinity of species I was 6–75-fold lower than that of native Hbα (R-state) and Mb.[51-53] This low affinity for O_2 was kinetically due to an 8–18-fold increase in $k_{off}^{O_2}$.

In Hb and Mb, the distal His-64 stabilizes bound O_2 due to the hydrogen bonding. Rohlfs *et al.* showed that replacement of His-64 in rMb with nonpolar amino acid residues (Leu or Phe) results in loss of hydrogen bonding and increases $k_{off}^{O_2}$ (342–833-fold higher than Mb).[53] In rHSA(double mutant)-heme, dioxygenated heme is buried in the core of the hydrophobic cavity without any counterpart for the hydrogen bond; thus the even small $k_{off}^{O_2}$ for species I are greater than those of Hbα and Mb. In species II, the proximal-side steric effect further enhanced the dissociation rates and caused large decline in O_2 binding affinity.

We compared O_2 and CO binding properties of the rHSA(I142H/Y161F)-heme and rHSA(I142H/Y161L)-heme and found an interesting distal-side steric effect on ligand binding.[41] The rHSA(I142H/Y161F)-heme complex binds O_2 and CO about 4–6 times more strongly than rHSA(I142H/Y161L)-heme, because of high association rate constants. This affect appears due to the concerted steric effects of the residues at positions 161 and 185. In the rHSA(I142H/Y161F)-heme complex, the bulky benzyl side-chain of Phe-161 (137 Å^3) may prevent rotation of neighboring Leu–185, thereby providing easy access of O_2 to the heme (**Fig. 5A**). In contrast, substitution of Phe-161 by the smaller Leu-161 (102 Å^3) may allow free rotation of the isopropyl group of Leu-185, which reduces the volume of the distal side (**Fig. 5B**) and hinders association of O_2 and CO with heme.

rHSA(triple mutant)-heme complexes with a distal base: HSA(I142H/Y161F)-heme and HSA(I142H/Y161L)-heme bind and release O_2, but their O_2 binding affinity is one order of magnitude lower than that of Hbα

Table 1. O_2 binding parameters of rHSA(mutant)-heme complexes in 50 mM potassium phosphate buffered solution (pH 7.0) at 22°C[a]

Hemoproteins	$k_{on}^{O_2}$ ($\mu M^{-1}s^{-1}$)	$k_{off}^{O_2}$ (ms^{-1})		$P_{1/2}^{O_2}$ (Torr)	
		I	II	I	II
rHSA(I142H/Y161F)-Heme	20	0.10	0.99	3	31
rHSA(I142H/Y161L)-Heme	7.5	0.22	1.70	18	134
rHSA(I142H/Y161F/L185N)-Heme	26	0.10	1.03	2	24
rHSA(I142H/Y161L/L185N)-Heme	14	0.02	0.29	1	14
rHSA(I142H/Y161L/R186L)-Heme	25	0.41	8.59	10	209
rHSA(I142H/Y161L/R186F)-Heme	21	0.29	7.01	9	203
Hbα (R-state)[b]	33[c]	0.013[d]		0.24	
Mb[e]	14	0.012		0.51	
RBC[f]				8	

[a]Number I or II indicates species I or II.[41,42] [b]Human Hb α-subunit. [c]In 0.1 M phosphate buffer (pH 7.0, 21.5°C).[51] [d] In 10 mM phosphate buffer (pH 7.0, 20°C).[52] [e]Sperm whale Mb. In 0.1 M potassium phosphate buffer (pH 7.0, 20°C).[53] [f]Human red cell suspension. In isotonic buffer (pH 7.4, 20°C)[62]

Table 2. CO binding parameters of rHSA(mutant)-heme complexes in 50 mM potassium phosphate buffered solution (pH 7.0) at 22°C[a]

Hemoproteins	k_{on}^{CO} ($\mu M^{-1}s^{-1}$)		k_{off}^{CO} (s^{-1})		$P_{1/2}^{CO}$ (Torr)	
	I	II	I	II	I	II
rHSA(I142H/Y161F)-Heme	6.8	0.72	0.009	0.061	0.0011	0.068
rHSA(I142H/Y161L)-Heme	2.0	0.27	0.013	0.079	0.0053	0.240
rHSA(I142H/Y161F/L185N)-Heme	7.7	1.09	0.008	0.043	0.0008	0.032
rHSA(I142H/Y161L/L185N)-Heme	6.8	1.60	0.008	0.039	0.0010	0.020
rHSA(I142H/Y161L/R186L)-Heme	5.0	0.57	0.011	0.165	0.0018	0.234
rHSA(I142H/Y161L/R186F)-Heme	7.9	1.12	0.010	0.148	0.0010	0.107
Hbα (R-state)[b]	4.6[c]		0.009[d]		0.0016[c]	
Mb[f]	0.51		0.019		0.030	

[a]Number I or II indicates species I or II.[41,42] [b]Human Hb α-subunit. [c]In 50 mM potassium phosphate buffer (pH 7.0, 20°C).[63] [d]In 0.1 M phosphate buffer (pH 7.0, 20°C).[61] [e]Calculated from $(k_{on}^{CO}/k_{off}^{CO})^{-1}$. [f]Sperm whale Mb. [d]In 0.1 M potassium phosphate buffer (pH 7.0, 20°C)[62]